The Pennsylvania State University
APPLIED RESEARCH LABORATORY
P.O. Box 30
State College, PA 16804

UNSTEADY FORCE CALCULATIONS IN TURBOMACHINERY

by

William C. Zierke

Technical Report No. TR 91-008
July 1991

Supported by:
Naval Sea Systems Command

L.R. Hettche, Director
Applied Research Laboratory

UNCLASSIFIED
SECURITY CLASSIFICATION OF THIS PAGE

REPORT DOCUMENTATION PAGE

1a REPORT SECURITY CLASSIFICATION Unclassified	1b. RESTRICTIVE MARKINGS
2a. SECURITY CLASSIFICATION AUTHORITY	3. DISTRIBUTION/AVAILABILITY OF REPORT Unlimited
2b DECLASSIFICATION/DOWNGRADING SCHEDULE	
4 PERFORMING ORGANIZATION REPORT NUMBER(S) TR-91-008	5. MONITORING ORGANIZATION REPORT NUMBER(S)
6a NAME OF PERFORMING ORGANIZATION Applied Research Laboratory 6b OFFICE SYMBOL (If applicable) ARL	7a. NAME OF MONITORING ORGANIZATION Naval Sea Systems Command Department of the Navy
6c ADDRESS (City, State, and ZIP Code) P. O. Box 30 State College, PA 16804	7b. ADDRESS (City, State, and ZIP Code) Washington, DC 20362
8a NAME OF FUNDING/SPONSORING ORGANIZATION Naval Sea Systems Command 8b OFFICE SYMBOL (If applicable) NAVSEA	9. PROCUREMENT INSTRUMENT IDENTIFICATION NUMBER
8c ADDRESS (City, State, and ZIP Code) Department of the Navy Washington, DC 20362	10. SOURCE OF FUNDING NUMBERS PROGRAM ELEMENT NO. / PROJECT NO. / TASK NO. / WORK UNIT ACCESSION NO.

11 TITLE (Include Security Classification)
Unsteady Force Calculations in Turbomachinery

12 PERSONAL AUTHOR(S)
William C. Zierke

13a TYPE OF REPORT	13b TIME COVERED FROM ____ TO ____	14. DATE OF REPORT (Year, Month, Day)	15. PAGE COUNT
		July 1991	49

16 SUPPLEMENTARY NOTATION

17 COSATI CODES			18. SUBJECT TERMS (Continue on reverse if necessary and identify by block number)
FIELD	GROUP	SUB-GROUP	

19 ABSTRACT (Continue on reverse if necessary and identify by block number)

This report gives a review of the various types of unsteady flow phenomena that occur within a turbomachine and examines existing methods for computing several of these flows. Then, we discuss a method for applying two-dimensional, unsteady, thin airfoil theory in a stripwise manner to compute the unsteady forces and moments on the shaft of a rotor operating within a nonuniform inflow. Techniques for computing these unsteady forces and moments on a rotor blade row with rake and skew are included.

20 DISTRIBUTION/AVAILABILITY OF ABSTRACT ☒ UNCLASSIFIED/UNLIMITED ☐ SAME AS RPT. ☐ DTIC USERS	21. ABSTRACT SECURITY CLASSIFICATION Unclassified
22a NAME OF RESPONSIBLE INDIVIDUAL	22b. TELEPHONE (Include Area Code) 814-865-6344 / 22c. OFFICE SYMBOL

DD FORM 1473, 84 MAR 83 APR edition may be used until exhausted. All other editions are obsolete.

SECURITY CLASSIFICATION OF THIS PAGE
Unclassified

Abstract

This report gives a review of the various types of unsteady flow phenomena that occur within a turbomachine and examines existing methods for computing several of these flows. Then, we discuss a method for applying two-dimensional, unsteady, thin airfoil theory in a stripwise manner to compute the unsteady forces and moments on the shaft of a rotor operating within a nonuniform inflow. Techniques for computing these unsteady forces and moments on a rotor blade row with rake and skew are included.

Table of Contents

List of Figures

Nomenclature

a_n	Fourier coefficients of the cosine terms
a_o	Fourier cosine amplitude of the zeroth harmonic
b_n	Fourier coefficients of the sine terms
B	number of rotor blades
c	rotor blade chord length
C	Theodorsen Function
C_L	steady lift coefficient
$\frac{dC_L}{d\alpha}$	slope of lift line
F	force on the rotor blade per unit span
F_f	maximum camber function
F_α	angle of attack function
i	$\sqrt{-1}$
J_o	Bessel Function of the first kind of order zero
J_1	Bessel Function of the first kind of order one
k	blade rate harmonic
ℓ	rotor blade index
L	lift force on the rotor blade per unit span
m	meridional direction
M	moment on the rotor blade per unit span
n	inflow harmonic
r	radius from the centerline of the turbomachine (radial direction)
s	rotor blade spacing

S	Sears Function
t	time
T	Horlock Function
u	distortion velocity parallel to the relative velocity ($\overline{W}$) (chordwise gust)
v	distortion velocity normal to the relative velocity ($\overline{W}$) (transverse gust)
V	absolute velocity
V_∞	freestream or advance velocity
W	velocity relative to the rotor blade
x	horizontal coordinate direction
x_b	coordinate direction parallel to the relative velocity ($\overline{W}$)
y	vertical coordinate direction
y_b	coordinate direction normal to the relative velocity ($\overline{W}$)
y_m	maximum camber of the blade
Y_o	Bessel Function of the second kind of order zero
Y_1	Bessel Function of the second kind of order one
z	axial coordinate direction
z_r	axial displacement of rotor blade section (rake)
α	angle of attack on rotor blade
α_{eff}	effective anlge of attack on rotor blade
β	absolute flow angle
γ	stagger angle of the rotor blade
δ_n	distortion amplitude variation factor
θ	angular coordinate direction
μ	streamline inclination angle $= \tan^{-1}(\overline{V}_r/\overline{V}_z)$
ν_n	angular frequency of the n^{th} harmonic
ρ	fluid density
τ_n	inter-blade phase angle

ϕ_n	distortion phase angle
Φ_n	unsteady lift phase angle on reference blade
ψ	angular displacement of rotor blade section (skew)
ω	reduced frequency
Ω	angular frequency of a rotor blade section

Subscripts

H	radial hub
m	meridional direction
mc	midchord
n	inflow harmonic order
	$= kB$, multiples of the number of rotor blades
	$= kB \pm 1$, adjacent to the multiples of the number of rotor blades
r	radial direction
T	radial tip
x	horizontal coordinate direction
y	vertical coordinate direction
x_{b_o}	located at position x_{b_o} along the chord
y_{b_o}	located at position y_{b_o} along the chord
z	axial coordinate direction
θ	angular coordinate direction

Superscripts

$\bar{}$	steady or circumferential average
$\tilde{}$	unsteady or circumferentially varying
$'$	rotating coordinate
$\rightarrow$	vector

Introduction

For many years, engineers have designed and analyzed turbomachines using one major assumption. They have assumed the flow to be steady. However, as we strive to design even better turbomachines, we must begin to focus on the complexities of unsteady flow. For various types of turbomachinery, unsteady flow can affect energy transfer, blade vibration, noise generation, heat transfer, and cavitation characteristics.

Before we discuss the unsteady flow considerations in turbomachinery design, we will briefly review the various types of unsteady flows in turbomachines. Given some knowledge of the physical phenomena involved, we shall examine several available methods for calculating unsteady forces and moments and how these methods can be applied to turbomachinery blading. We shall discuss the advantages and disadvantages of all these methods as well as point out the approximations needed in the development of these methods. Finally, we show how we can adapt these methods to turbomachinery.

Unsteady Flows in Turbomachines

Before we include unsteady effects in our design process, we must begin to understand the physics of these various unsteady effects and the relationship between these various effects. Dean [1959] showed that the flow through a turbomachine had to be unsteady. His "unsteady paradox" states that local unsteady changes in static pressure must exist within a turbomachine in order for that machine to exchange energy with the fluid. If this turbomachine includes only a single blade row with a uniform inflow, we can consider the problem to be steady by writing our governing equations in a coordinate system rotating with the blades. When a row of rotating blades operates with a circumferentially varying inflow, or if it operates in the vicinity of stationary blades, struts, or other appendages–the flow is unsteady, despite the frame of reference we use.

When we discuss unsteady flow in turbomachinery, we usually refer to periodic unsteadiness. We must also remember that a random or aperiodic unsteadiness exists because of turbulence. Turbulence also has strong effects on energy and heat transfer and it also includes important random pressure fluctuations. Our concern with turbulence will be in how turbulence interacts with periodic unsteadiness.

Let us now discuss why an inherent periodic unsteadiness exists within a turbomachine. Blades moving relative to one another can operate within a periodically varying potential flow field. For incompressible flows, we can normally neglect this periodic potential interaction when a blade row is displaced at least one chord length upstream or downstream of neighboring rows of blades or appendages. For compressible flows, the influence of the periodic potential field extends much farther axially as the Mach number increases.

Because of the fairly large axial blade gaps in most turbomachines, the periodic potential interactions are usually dominated by other types of periodic unsteadiness. Most importantly,

a blade row interacts with the wakes shed from an upstream row of blades or appendages that have relative motion. These wakes are convected downstream, chopped by the downstream blade row, and transported through the downstream blade passages. As seen in Figure 1, the periodically passing wakes cause a periodically varying incidence angle on the downstream blades. This unsteady incidence results in a periodically varying blade static-pressure distribution and thus a periodically varying lift. In addition, the behavior of the chopped wake segment as it is transported through the blade passage is quite interesting. For instance, we can see from Figure 2 that the highly turbulent fluid in the wake segment moves from the suction surface of a compressor blade and impinges on the pressure surface as the wake segment moves downstream. This action results in local pressure fluctuations due to the passing wake segment. Meyer [1958] made the first theory of this wake interaction effect while Kerrebrock and Mikolajczak [1970] proved it experimentally. For a turbine blade passage, the wake fluid moves from the pressure surface to the suction surface. Other researchers have further extended our knowledge of wake interaction effects.

Periodic wake interactions have many influences that can affect a turbomachine design. The periodically varying blade static-pressure distribution can cause a forced vibration. Unsteady forces and moments affect the blades and whatever is attached to the blades such as the rotor shaft or the stationary hub and casing. These unsteady forces can cause vibration at the frequency of unsteadiness–namely the blade rate frequency and its harmonics. Periodic wake interactions also cause the boundary layers near the blade surface to be unsteady. Varying the blade static-pressure distribution changes the local streamwise pressure gradients which in turn changes the boundary layer characteristics. In addition, the effects of the transported wake segments can have strong local effects on the boundary layer. Evans [1978], Walker [1982], and Hodson [1983] all made measurements within turbomachines that show some boundary layers alternating between laminar and turbulent because of the unsteady flow. Periodic unsteadiness can also affect separation. These unsteady boundary layers, along with the complexities of the wake interactions,

strongly affect the energy transfer within the machine. In addition, the changing character of the boundary layers affects the turbulence and thus the random pressure fluctuations. Finally, if the pressure fluctuations become large enough, cavitation can occur in machines operating with liquid as the working fluid–as shown by the unsteady cavitation experiment of Yeh and Eisenhuth [1959].

A few other characteristics of periodic wake interactions should be noted. First, time or phase lags always appear. As the incidence angle changes, the static pressure near the leading edge of the blade changes much sooner than the static pressure near the trailing edge. In fact, experiments have shown that the amplitude of the periodically changing pressure is much larger near the leading edge than near the trailing edge. The effect of the varying incidence appears to decay as one approaches the trailing edge. In addition, the characteristics of the unsteady boundary layers can also lag behind the change in the local velocity and static-pressure gradient. We should also take note of a second important factor. The flow within the wakes and wake segments can also be unsteady. We have all seen measurements that make us think of a wake as merely a region of velocity defect. However, these measurements are probably time-average measurements. In fact, real turbomachine wakes can be made of periodically unsteady vortex streets such as those we normally identify with the wakes behind blunt bodies. This wake unsteadiness includes time varying pressures which can influence the unsteady wake interactions.

In addition to the periodically unsteady potential and wake interactions, we can encounter other kinds of periodically unsteady flows. Blades may also periodically interact with shock waves, end-wall boundary layers, tip vorticies, and other secondary flow vorticies. The three-dimensional nature of these types of flow can create significant circumferential variations in velocity and static pressure which interact unsteadily with downstream blades.

We have only discussed unsteady flows that are inherently found in turbomachine flows. Since these flows will always exist, we must learn their effects and use this knowledge to design better turbomachines. Other types of unsteady flows can occur, however, which we must try to

avoid. These unsteady flows are instabilities which may cause large resonant stresses in blades and drastic reductions in machine performance.

As blades vibrate, the mechanical surfaces exchange energy with the fluid passing through the blade passage. If the fluid extracts energy from the blade, the surface oscillations will be aerodynamically dampened. However, if the fluid increases the energy of the oscillating blades, the blades will become vibrationally unstable. We call this instability flutter. Flutter exists because the unsteady work on the blades exceeds the work dissipated by friction and material damping. Normally, flutter occurs when the blade boundary layer separates. But flutter can also occur when the blade boundary layers are attached–especially at near-choke conditions. Compressibility strongly increases the chances of developing flutter.

Large inlet flow distortions can cause a blade to stall in a turbomachine in a similar manner in which an isolated blade may stall. In both cases, the potential flow around the blade will change. In a turbomachine, however, the new potential flow will decrease the incidence of one neighboring blade and will increase the incidence of the other adjacent blade, causing this blade to stall. A stall zone of one or more blade passages will then propagate circumferentially around the annulus of blades. We call this flow instability rotating stall and it leads to a large pressure drop across the blade passage. Hysteresis effects cause the recovery from rotating stall to be very difficult. For machines where the working fluid is liquid, inlet flow distortions and the corresponding changes in incidence angle can lead to cavitation. Some machines have shown an instability similar to rotating stall called rotating cavitation.

Rotating stall is one factor that can lead to a global instability within a compressor called surge. Surge occurs when the throttle pressure-loss characteristic curve has a smaller slope than the constant-speed compressor characteristic curve at the point of operation. A reduction in flow would then cause a greater reduction in compressor pressure rise than the corresponding pressure drop through the throttling system. As a result, the annulus mass flow oscillates with large changes in amplitude at low frequencies.

Reduced Frequency

Periodic unsteady flow can have strong effects on a turbomachine, but the strength of these effects varies with the level of unsteadiness. Therefore, we need some parameter that represents the level of unsteadiness.

The level of unsteadiness depends on two time scales. First, the time scale associated with the angular frequency of the unsteady motion relative to the rotating blades is $\frac{1}{\nu_n}$. For this case, our interest is in the n^{th} harmonic of the unsteady motion. Second, we need the time scale associated with the time it takes a fluid particle to travel through the device. If this device is a blade row, a fluid particle will travel through the blade passage in time $\frac{c}{W}$. The ratio of these time scales then describes the change in local flow parameters while a fluid particle resides in a blade passage. If we change the relevant length from c to $\frac{c}{2}$, we refer to this ratio as the reduced frequency,

$$\omega_n = \frac{\nu_n c}{2W} .$$

Sometimes c is used instead of $\frac{c}{2}$. We could also think of the reduced frequency as a ratio of length scales–the semi-chord divided by the wavelength of the n^{th} harmonic of the unsteady motion.

For many unsteady flow problems, such as the periodic shedding of vorticies into a wake, one refers to the reduced frequency as a Strouhal number (see Strouhal [1878]). For the problem of a shedding Karman vortex street, we might substitute the shedding frequency for ν_n and the trailing edge diameter for $\frac{c}{2}$ in defining a Strouhal number. For periodic interaction problems in turbomachinery, we use the reduced frequency where the disturbance is both moving circumferentially relative to a blade row and is being convected downstream.

For a reduced frequency much less than one, we refer to the unsteady flow as quasi-steady. That is, the flow is only a function of the instantaneous conditions and not a function of previous conditions. For a reduced frequency greater than one, the limiting state of quasi-steady flow would provide estimates of the unsteady flow that would be much too conservative. Most turbomachinery flows are characterized by reduced frequencies of order unity or greater and we cannot adequately describe these flows in a quasi-steady manner. In compressible flow, the level of unsteadiness depends on the product of the reduced frequency and the Mach number.

In turbomachinery problems, we may require an additional nondimensional frequency parameter. Once again, we need the time scale associated with the angular frequency of the unsteady motion relative to the rotating blades, $\frac{1}{\nu_n}$. Next, we need the time scale associated with the motion of the blades relative to the distortion, $\frac{s}{r\Omega}$. Taking the ratio gives

$$\tau_n = \frac{\nu_n s}{r\Omega} = 2\omega_n \left(\frac{s}{c}\right) \left(\frac{\overline{W}}{r\Omega}\right) .$$

We call this nondimensional parameter the inter-blade frequency or the inter-blade phase angle. This parameter accounts for the variation in unsteady interactions from blade to blade. Just as we think of ω_n as a ratio of semi-chord to disturbance wavelength, we can think of τ_n as a ratio of blade spacing to disturbance wavelength.

Unsteady Singularity Solutions

Several different types of methods exist for computing the unsteady forces and moments on a turbomachine blade. As we have already discussed, we can use quasi-steady methods for flows with a reduced frequency much less than one. We assume that the blades operate continually at the instantaneous flow conditions. Then we can calculate the unsteady forces by actually calculating the steady forces at each instant of time. An example is a quasi-steady actuator disc analysis. One of the oldest methods for computing unsteady forces and moments involves the modeling of the blades with singularities and letting the singularities induce a potential flow around the blade. Another method involves the treatment of the blades as boundaries and modeling the flow with the governing partial differential equations of fluid mechanics. These partial differential equations are further approximated and solved numerically.

Interest in the use of singularity solutions for unsteady flow problems began in the 1930's. Theodorsen [1935] derived the exact solution for a flat plate in sinusoidally oscillatory motion. Von Karman and Sears [1938] used the ideas of Theodorsen [1935] for their unsteady thin airfoil theory and finally Sears [1941] expanded these ideas to derive his unsteady lift function. The unsteady thin airfoil theory of Sears [1941] has many similarities with steady thin airfoil theory for incompressible flow. Sears [1941] represented an airfoil as a flat plate of zero thickness and modeled the airfoil with a continuous vortex distribution along its chord. Each vortex induces a potential flow at every point in the flow field which we can superimpose upon the potential flow from the steady inflow. Unfortunately, the system of equations is not closed since the downstream conditions remain unknown. We can complete the solution and find a unique lift by applying the Kutta condition; no velocity discontinuity can exist at the trailing edge. Now we adjust the strength of the vortex distribution such that no fluid flows through the airfoil giving the airfoil

a unique bound vorticity and lift. For his unsteady problem, Sears [1941] treated the inflow as a gust being convected with a velocity, $\overline{W}$. Figure 3 shows this gust which we assume as a harmonic function in time. Sears [1941] assumed that the amplitude of the disturbance velocity normal to the chord ,$\tilde{v}$, is small compared to $\overline{W}$.

Sears [1941] found it necessary to expand on the Kutta condition when applying it to unsteady flow. Since the inflow varies in time, the strength of the vortex distribution necessary to satisfy the blade boundary condition will also vary with time; this then causes the lift to vary with time. Thus, a trailing vorticity must be shed into the wake. The trailing vorticity affects the flow throughout the flow field which means that the flow field depends on the history of the periodically unsteady flow. Sears [1941] modeled the trailing vorticity with a vortex distribution being convected away from the airfoil in the direction of the chord with a velocity, $\overline{W}$.

Sears [1941] developed an equation for the unsteady lift per unit span, $\tilde{L}_n$, for a transverse disturbance velocity, $\tilde{v}_n$, and a reduced frequency, ω_n,

$$\tilde{L}_n(t) = \frac{1}{2}\frac{dC_L}{d\alpha}\rho c\overline{W}\tilde{v}_n\, S(\omega_n)$$

where

$$S(\omega_n) = C(\omega_n)\,[J_0(\omega_n) - i\,J_1(\omega_n)] + i\,J_1(\omega_n)$$

is called the Sears Function. Theodorsen [1935] developed

$$C(\omega_n) = \frac{J_1(\omega_n) - iY_1(\omega_n)}{[J_1(\omega_n) - iY_1(\omega_n)] + i[J_0(\omega_n) - iY_0(\omega_n)]}$$

which we call the Theodorsen Function. We calculate unsteady lift functions of this kind from Bessel functions using the appropriate reduced frequency. We should note that several of the singularity techniques under discussion were developed for isolated, thin airfoils with infinite span where the theoretical value of $\frac{dC_L}{d\alpha}$ equals 2π. Since we are concerned with nonisolated turbomachinery blades with finite span and thickness, we will let $\frac{dC_L}{d\alpha}$ remain a variable. Osborne

[1973] made a further modification. He developed an unsteady thin airfoil theory for transverse gusts that includes compressibility effects.

Since the inflow gust varies harmonically in time, all the time varying quantities will be harmonic functions which we associate with an amplitude and a phase angle. We can then plot the Sears Function on the complex plane as done in Figure 4. For a very small ω_n, $S(\omega_n)$ lies near the real axis giving a small phase angle and showing why a quasi-steady approach works. For increasing ω_n, the entire airfoil cannot respond immediately to a changing incidence which results in a significant phase angle.

Horlock [1968a] extended the unsteady thin airfoil theory to include a steady angle of attack and thus a chordwise gust, $\tilde{u}_n$,

$$\tilde{L}_n(t) \;=\; \frac{1}{2}\frac{dC_L}{d\alpha}\rho c\overline{W}\,[\tilde{v}_n\,S(\omega_n) \;+\; \alpha\tilde{u}_n\,T(\omega_n)]$$

where

$$T_n(\omega) \;=\; J_0(\omega_n) \;+\; i\,J_1(\omega_n) \;+\; S(\omega_n)$$

is termed the Horlock Function. Holmes (see Horlock [1968b]) and Naumann and Yeh [1973] further extended the unsteady thin airfoil theory to include camber,

$$\tilde{L}_n(t) \;=\; \frac{1}{2}\frac{dC_L}{d\alpha}\rho c\overline{W}\left[\tilde{v}_n\,S(\omega_n) \;+\; \alpha\tilde{u}_n\,F_\alpha(\omega_n) \;+\; \frac{2y_m\tilde{u}_n}{c}\,F_f(\omega_n)\right]$$

where

$$F_\alpha \;=\; J_0(\omega_n) \;+\; i\,J_1(\omega_n)$$

and

$$F_f \;=\; 3\,J_2(\omega_n) \;+\; J_0(\omega_n) \;+\; C(\omega_n)\,[J_0(\omega_n) \;-\; J_2(\omega_n) \;-\; i\,2\,J_1(\omega_n)]\;.$$

They obtained this equation by placing the vortex distribution on the camber line, but with a small value of camber such that the blade boundary condition could be satisfied along the chord line. We should note that these new unsteady lift functions are merely added to the Sears Function. To obtain this result, we must assume small values of steady lift, steady angle of

attack, and maximum camber. We also need to assume small values of $\tilde{u}_n$ and $\tilde{v}_n$ as compared to $\overline{W}$. These assumptions allow us to linearize the various potential flow equations and obtain $\tilde{L}_n$ as the summation of various functions.

Before we use these versions of the unsteady thin airfoil theory for turbomachinery problems, we must determine the correct reduced frequency associated with the various Bessel functions. For the case of a blade rotating through a nonuniform inflow, Figure 5 shows the n^{th} harmonic of an inflow distortion convected with an absolute flow angle β. For $\beta = 0$, the distortion lies in the circumferential direction and has a wavelength of $\left(\frac{2\pi r}{n}\right)$. For a nonzero value of β, the wavelength becomes $\left(\frac{2\pi r}{n}\right) \sec(\beta)$. However, we must model this distortion as a transverse gust and a chordwise gust in order to apply unsteady thin airfoil theory.

As shown in Figure 5, we can decompose this distortion into two components–both perpendicular and parallel to the blade chord. In order to determine the correct reduced frequency associated with these two gusts, we first must compute the angular frequency,

$$\nu_n = 2\pi \frac{\text{phase velocity}}{\text{wavelength}} .$$

The phase velocity for the transverse (or perpendicular) gust is the component of the relative velocity vector, $\overline{W}$, in the chordwise direction. As mentioned earlier, the chorwise (or parallel) gust will only produce an unsteady lift if the blade experiences a steady angle of attack or if the blade has camber. The phase velocity will be the component of $\overline{W}$ perpendicular to the chord. When α is zero, this will give a phase velocity of zero and, therefore, values of zero for the angular frequency, reduced frequency, and unsteady lift–which we know cannot be the case for a cambered blade. To circumvent this problem, we can determine an effective angle of attack, α_{eff}, by adding the angle of zero lift to the angle of attack. The zero lift line can be approximated as passing through the trailing edge and the camber line at midchord. Further, assuming that the value of camber at midchord is y_m yields

$$\alpha_{\text{eff}} = \alpha + \tan^{-1}\left(\frac{2y_m}{c}\right) .$$

We can compute a wavelength for the transverse gust of $\left(\frac{2\pi r}{n}\right)\csc(\gamma)$ and the chordwise gust of $\left(\frac{2\pi r}{n}\right)\sec(\gamma)$. From this information, we can now find the angular frequency of the unsteady transverse gust relative to the rotating blade,

$$\nu_n = 2\pi\left[\frac{\overline{W}\cos(\alpha_{\text{eff}})}{\left(\frac{2\pi r}{n}\right)\csc(\gamma)}\right] = \left(\frac{n\overline{W}}{r}\right)\sin(\gamma)\cos(\alpha_{\text{eff}}) ,$$

and a reduced freqency,

$$\omega_n = \left(\frac{nc}{2r}\right)\sin(\gamma)\cos(\alpha_{\text{eff}}) .$$

The angular frequency of the unsteady chordwise gust relative to the rotating blade is

$$\nu_n = 2\pi\left[\frac{\overline{W}\sin(\alpha_{\text{eff}})}{\left(\frac{2\pi r}{n}\right)\sec(\gamma)}\right] = \left(\frac{n\overline{W}}{r}\right)\cos(\gamma)\sin(\alpha_{\text{eff}})$$

and the reduced freqency is

$$\omega_n = \left(\frac{nc}{2r}\right)\cos(\gamma)\sin(\alpha_{\text{eff}}) .$$

In evaluating the various lift functions, we need to use the appropriate reduced frequency corresponding to either the transverse or chordwise gust.

Aside from the assumptions already stated, Horlock [1968a], Holmes (see Horlock [1968b]), and Naumann and Yeh [1973] also assumed that the incoming gust would not change as it was convected past the airfoil. Goldstein and Atassi [1976] allowed the gust to be distorted by the steady-state potential flow field about the airfoil. This coupling effect led to a second-order expansion for calculating the unsteady lift about the airfoil. Atassi [1984] expanded these ideas to show that the resulting expressions for the unsteady lift still possess a linear character.

We have discussed several methods to model the unsteady wake interaction problem. By treating the oncoming wakes as time-dependent gusts, these models attempt to model how the oncoming wakes periodically change the incidence of an isolated airfoil. None of these models accounts for the physics of the chopped wake segments within the blade passage. Meyer [1958] and Lefcort [1965] attempted to model this behavior. They modeled the chopped wake segments as jets sucking fluid from the suction surface of a compressor blade and impinging fluid on the

pressure surface. They then calculated the unsteady static pressure on an isolated thin airfoil in much the same manner as Sears [1941] except the modeled wake segments gave large local variations in static pressure. The contribution of Lefcort [1965] allowed for a more realistic wake width in the model.

So far, we have only discussed the use of unsteady thin airfoil theory to model the unsteady wake interaction problem. Kemp and Sears [1953] and more recently Lienhart [1974] have used unsteady thin airfoil theory to model the unsteady potential flow interaction as well. Kemp and Sears [1953] attempted to solve the unsteady interaction problem of a row of stator blades followed by a row of rotor blades. To avoid a very complex mathematical problem, they made several assumptions. The unsteady lift of a single stator depended only on the relative motion between that blade and the steady potential flow fields of the rotor blades. The unsteady lift of a single rotor blade depended on two things. First, the unsteady lift depended on the relative motion between that blade and the steady potential flow fields of the stator blades. Also, the unsteady lift on each rotor blade was computed using the upstream stator blade wakes with a theory similar to that of Sears [1941].

Kemp and Sears [1953] developed the first singularity technique for use with multiple blades. However, when calculating the unsteady lift of a particular blade, they neglected the unsteady effects from all other blades. As the solidity of a blade row increases, the neighboring blades have a stronger influence on the unsteady lift of the reference blade. We can make a slightly better assumption of the unsteady lift by using the method of Weinig [1935]. He computed the values of steady lift in cascades of various solidities and stagger angles which allows us to change the value of $\frac{dC_L}{d\alpha}$ (a quasi-steady correction). This method does break down for high stagger angles, however.

Some researchers have developed unsteady cascade analyses using unsteady thin airfoil theory. Whitehead [1960] modeled all of the blades with a finite number of vorticies (usually eight) and all of the trailing vortices with a continuous vortex distribution. Fleeter [1973] updated this

method to include the effects of compressibility. Whitehead [1960] also considered the vibrational response of each blade to the unsteady lift and Smith [1971] used this with some compressibility effects to determine the resulting acoustic field. For unsteady cascade analyses, we need the inter-blade frequency,

$$\tau_n = 2\omega_n \left(\frac{s}{c}\right) \left(\frac{\overline{W}}{r\Omega}\right) .$$

The strength of the bound and trailing vorticity from all blades must be summed and this sum must satisfy the unsteady blade boundary condition. In the development of his analysis, Whitehead [1960] uses a summation method that excludes solutions when τ_n equals an integer multiple of 2π. Therefore, his analysis does not solve cases where the number of cycles in the distortion (the inflow harmonic) is a multiple of the number of blades. After some complex integration, Whitehead [1960] computes an unsteady lift coefficient which we may use to replace the Sears Function in the unsteady lift equation of Naumann and Yeh [1973].

Henderson [1972] also developed an unsteady cascade analysis. He modeled the reference blade with a continuous vortex distribution and the other blades with a single vortex located at the quarter chord. Like Whitehead [1960], Henderson [1972] also modeled the trailing vortices with continuous vortex distributions. For turbomachinery problems, we should note that modeling the trailing vorticity along the extended chord line can become a poor assumption. Unfortunately, Henderson [1972] could not determine an analytical solution for one of the integrals in his analysis and therefore, he could not obtain a close-form solution.

Lienhart [1974] extended the potential interaction work of Kemp and Sears [1953] to include some vortex representation of all the blades. Thus, when calculating the unsteady lift on a blade, he included the unsteady effects due to all the other blades. However, he did not include unsteady wake interaction. Of these cascade analyses, only Henderson [1972] includes the effects of camber or steady angle of attack.

For us to apply the preceding singularity techniques to the turbomachinery problem, we must calculate the unsteady lift at several blade sections in two-dimensional, independent strips. In a

later section, we shall discuss the proper technique for summing unsteady forces and moments in a turbomachine using two-dimensional, unsteady strip theory.

Three-dimensional singularity techniques, although mathematically more complex, have also been developed. Brown [1964] developed an unsteady lifting line technique. As with lifting line methods for steady flow, a single vortex models each blade section and all of these vorticies form a continuous radial vortex distribution. Again, the strength of this distribution changes in time with the varying inflow resulting in shed vorticity downstream of the blade. Brown [1964] uses corrections to account for the bound vortex on neighboring blades and both the radial and streamwise trailing vorticity. For high reduced frequencies where the wavelength of the disturbance is much smaller than the chord, we might suspect that modeling each blade section with a single vortex will not give as enough resolution to properly calculate the unsteady lift. In order to somewhat alleviate this problem, we could model each blade section with several vorticies and thus model each three-dimensional blade with several lifting lines. We call this technique an unsteady *lifting surface technique*. Tsakonas, Jacobs, and Ali [1973], Kerwin and Lee [1978],and Tsakonas, Jacobs, and Liao [1983] have developed such unsteady lifting surface techniques. The latter two techniques consider moderately loaded blades where the discrete lifting lines lie on the camber surface. Kerwin and Lee [1978] also include sources in their singularity technique to account for blade thickness. The shed trailing vorticity travels on a helicoidal path downstream and the various unsteady lifting surface techniques differ on how to model this complex, three-dimensional phenomenon.

Unsteady Computational Fluid Dynamics

Unsteady singularity techniques have several drawbacks. First, we cannot adequately model many blades of interest in turbomachinery. Singularities cannot give us good surface definition (unless someone develops a good unsteady, three-dimensional panel method) and most methods limit the camber, thickness, and steady angle of attack. We also have difficulties modeling the shed trailing vorticity, the chopped wake segment effects, and some three-dimensional effects. Finally, since the singularities can only induce potential flow, we cannot extend these methods to viscous flow. It seems that much of our future unsteady flow computations will lie in numerically modeling the fluid flow instead of modeling the blades.

Several unsteady numerical methods have recently been developed. After much initial work by several researchers, Hodson [1985] developed a numerical method to compute the wake-generated unsteady flow around a rotating blade row. He modeled the two-dimensional, compressible, Euler equations and solved them using an explicit finite volume approach. Figure 6 shows some typical results for a turbine rotor row. These results show much of the anticipated physics of wake interactions. The unsteady static-pressure distribution may be numerically integrated to find the amplitude, phase angle, and location of the unsteady lift. Koya and Kotake [1985] developed a similar method. They do everything the same as Hodson [1985] except that they apply the method to the three-dimensional, compressible, Euler equations. They have also attempted to apply the method to successive blade rows to obtain the unsteady potential flow effects. However, since the method is inviscid, they cannot compute the wakes from the upstream blade row that interact with the downstream blade row.

We still have many problems that hinder our use of unsteady computational fluid dynamics in computing unsteady forces and moments in turbomachines. When applying Euler solvers to the

steady cascade problem, we use spatial periodicity in our boundary conditions. In the unsteady cascade problem, we can either use time-dependent periodicity conditions or we must include the number of blade passages over which the upstream flow pattern repeats. These alternatives are either difficult to apply or very time consuming. Also, we must generate a suitable grid. For the multiple blade row problem, the grids for each blade row must coincide at each time step. Additionally, we might have a simple bookkeeping and computer storage problem since the computations must include enough time steps to include the transient period and at least one cycle of the periodic unsteady flow. Finally, no adequate computational methods exist yet for the incompressible, unsteady flow problem.

Several methods exist for computing unsteady boundary layer flows. Most of these methods simply use the unsteady, two-dimensional, boundary layer equations. A major problem occurs when attempting to use these methods in turbomachinery problems since these boundary layers have regions of laminar, transitional, turbulent, and separated flow. We find the biggest problem in our selection of a turbulence model. Modeling Reynolds stresses is difficult enough in steady, viscous flow. For unsteady flow, we can obtain Reynolds stresses due to periodic unsteadiness as well as turbulent unsteadiness. Furthermore, our selection of empirical constants for these turbulence models becomes more difficult because of the interaction between the periodic and turbulent unsteadiness. Besides, few if any good periodic unsteady experiments exist for the selection of these constants.

Nonuniform Inflow

Before we compute the unsteady forces and moments within a turbomachine, we need to establish the nonuniform flow upstream of the blade row of interest. We can compute the nonuniform inflow by numerically solving the viscous flow around the blades creating the wakes, or we can use some numerical method in conjunction with some empirical wake models. However, in order to satisfactorily obtain the entire harmonic content of the nonuniform inflow, we may need to measure the wakes experimentally. In any case, we must be aware that the flow field experienced by a rotating blade row will be different than the flow field that exists with the rotating blade row removed. Since the rotor blades accelerate the flow, the rotor blades will shift the streamlines toward the roots of the rotor blades in order to satisfy continuity.

If we intend to compute the unsteady forces and moments with a singularity technique, we need to simulate the nonuniform inflow as a convected gust. We can consider any nonuniform inflow as a harmonic function in space. First, we decompose the nonuniform inflow into a circumferential average velocity and a circumferentially varying velocity,

$$V(z,r,\theta) \;=\; \overline{V}(z,r) \;+\; \widetilde{V}(z,r,\theta)\;.$$

We may describe this velocity by a Fourier series as

$$V(z,r,\theta) \;=\; \frac{a_0}{2} \;+\; \sum_{n=1}^{\infty} \left[a_n \cos(n\theta) \;+\; b_n \sin(n\theta)\right]$$

where

$$a_n(z,r) \;=\; \frac{1}{\pi}\int_{-\pi}^{\pi} V \cos(n\theta)\, d\theta$$

and

$$b_n(z,r) \;=\; \frac{1}{\pi}\int_{-\pi}^{\pi} V \sin(n\theta)\, d\theta\;.$$

The term $\frac{a_0}{2}$ represents the circumferential average velocity, $\overline{V}$. We can now rewrite the distortion velocity for the n^{th} harmonic as

$$\begin{aligned}
\widetilde{V}_n(z,r,\theta) &= a_n \cos(n\theta) + b_n \sin(n\theta) \\
&= |\widetilde{V}_n|\,(a_n/|\widetilde{V}_n|) \cos(n\theta) + |\widetilde{V}_n|\,(b_n/|\widetilde{V}_n|) \sin(n\theta) \\
&= |\widetilde{V}_n| \cos(\phi_n) \cos(n\theta) + |\widetilde{V}_n| \sin(\phi_n) \sin(n\theta) \\
&= |\widetilde{V}_n| \cos(n\theta - \phi_n)
\end{aligned}$$

where $|\widetilde{V}_n|$ represents the amplitude of the distortion velocity and ϕ_n represents the phase angle. The phase angle represents the combination of cosine and sine waves that make up the n^{th} harmonic. We can define the amplitude and phase angle as

$$|\widetilde{V}_n|(z,r) = \sqrt{a_n^2 + b_n^2}$$

and

$$\phi_n(z,r) = \tan^{-1}(b_n/a_n) \, .$$

We define the phase angle as positive when measured in the direction opposite to blade rotation. It is also important to know the θ position where the measured phase angle was referenced. A typical reference position might be vertically up. We must also remember that all amplitudes and phase angles can vary radially and these variations can lead to changes in unsteady forces. For simplicity, we will rewrite the distortion as an exponential,

$$\widetilde{V}(z,r,\theta) = |\widetilde{V}_n|\, e^{i(n\theta - \phi_n)} \, .$$

In writing the distortion in this manner, we are only concerned with the real part of the expression.

Unsteady Forces and Moments on a Rotating Shaft

We will now focus on the calculation of unsteady forces and moments on a rotating shaft caused by rotor blades interacting with a nonuniform inflow. In order to accomplish this calculation, we will need to transfer the nonuniform inflow into a rotating coordinate system. For the interaction of a stator blade row with upstream rotor wakes, the rotating rotor wakes can be transferred into a stationary coordinate system. In either case, we need to adjust the distortion velocity in order to apply a two-dimensional, unsteady thin airfoil theory to a blade.

The distortion velocity will depend on the meridional direction[1], m. The fluid flows meridionally a distance m in time $\frac{m}{\overline{V}_m}$. In this time, the fluid also moves circumferentially a distance $r\Delta\theta$. Moving $r\Delta\theta$ takes time $\frac{r\Delta\theta}{\overline{V}_\theta}$. Since these two times must be equal, we obtain

$$\Delta\theta = \frac{m\overline{V}_\theta}{r\overline{V}_m} .$$

Thus, if swirl exists upstream of the rotating blades, the phase angle will vary meridionally:

$$\tilde{V}_n(z,r,\theta) = |\tilde{V}_n| e^{i\left[n\left(\theta - \frac{m\overline{V}_\theta}{r\overline{V}_m}\right) - \phi_n\right]} .$$

We can estimate the m dependence of $|\tilde{V}_n|$ with a factor $e^{-\delta_n m/\overline{V}_m}$. δ_n is a factor, in units of 1/sec, that shows how the distortion amplitude changes as m increases. One example of how $|\tilde{V}_n|$ can change meridionally is the diffusion of a wake due to viscosity. Thus

$$\tilde{V}_n(z,r,\theta) = |\tilde{V}_n| e^{-\delta_n m/\overline{V}_m} e^{i\left(n\theta - \phi_n - \frac{n\, m\overline{V}_\theta}{r\overline{V}_m}\right)} .$$

---

[1] The meridional direction is defined by the direction of the vector sum of the axial and radial mean velocities.

Since most analytical techniques compute the unsteady lift on an isolated airfoil, or at least reference the computation to a particular blade, we shall include a shift in the θ position due to the rotor blade number, B,

$$\widetilde{V}_n(z,r,\theta,\ell) \;=\; |\widetilde{V}_n|\, e^{-\delta_n m/\overline{V}_m}\, e^{i\left[n\left(\theta + \frac{2\pi\ell}{B}\right) - \phi_n - \frac{n\,m\overline{V}_\theta}{r\overline{V}_m}\right]} .$$

In order to calculate the unsteady lift on a rotor blade, we must shift from the stationary coordinate system that we have been using to a coordinate system rotating with the blades. Using Figure 7, we see that we must transform from (z,r,θ) to (z',r',θ') by

$$\theta \;=\; \theta' \;+\; \psi_{mc} \;-\; \Omega t \;,$$

$$z \;=\; z' \;+\; z_{r_{mc}} \;,$$

and

$$r \;=\; r' \;.$$

ψ_{mc} is the skew angle of the blade midchord, Ω is the angular velocity of the blades, and $z_{r_{mc}}$ is the rake of the blade midchord. The reference point of Figure 7 could represent a radial stacking line or a radial line defining the midchord rake and skew to be zero at the hub. We define the skew angle as positive in the direction opposite to blade rotation and rake as positive in the same direction as axial flow. Assuming that $z_{r_{mc}}$ is in the meridional direction instead of the axial direction (since $z_{r_{mc}}$ is usually small), we can now write the distortion velocity in terms of the rotating coordinate system

$$\widetilde{V}_n(z',r',\theta',t,\ell) \;=\; |\widetilde{V}_n|\, e^{-\delta_n(m' + z_{r_{mc}})/\overline{V}_m}$$
$$e^{i\left(-n\Omega t + \frac{n2\pi\ell}{B} - \phi_n + n\psi_{mc} - \frac{n\,z_{r_{mc}}\overline{V}_\theta}{r'\overline{V}_m} + n\theta' - \frac{n\,m'\overline{V}_\theta}{r'\overline{V}_m}\right)} .$$

In order for us to view the problem as time increases, we can simply change the sign of all the terms in the last exponential function. This will not change our results since we are only concerned with the real part of the expression. This yields

$$\widetilde{V}_n(z',r',\theta',t,\ell) \;=\; |\widetilde{V}_n|\, e^{-\delta_n(m' + z_{r_{mc}})/\overline{V}_m}$$
$$e^{i\left(n\Omega t - \frac{n2\pi\ell}{B} + \phi_n - n\psi_{mc} + \frac{n\,z_{r_{mc}}\overline{V}_\theta}{r'\overline{V}_m} - n\theta' + \frac{n\,m'\overline{V}_\theta}{r'\overline{V}_m}\right)} .$$

We note here that the measured phase angle, ϕ_n, causes a time lead and the skew angle causes a time lag in the distortion relative to the case with no measured phase and no skew. The rake, however, causes a time lead if $\overline{V}_\theta$ is positive and a time lag if $\overline{V}_\theta$ is negative.

Many analytical methods for computing the unsteady lift use a coordinate system (x_b', y_b', r') attached to the rotor blade as seen in Figure 7. We can rotate our current coordinate system to this rotating system using the following relations:

$$m' = x_b' \cos(\gamma + \alpha) - y_b' \sin(\gamma + \alpha)$$

and

$$r'\theta' = x_b' \sin(\gamma + \alpha) + y_b' \cos(\gamma + \alpha) .$$

From the velocity diagram of Figure 7, we obtain

$$\sin(\gamma + \alpha) = \frac{\overline{V}_\theta + r'\Omega}{\overline{W}}$$

and

$$\cos(\gamma + \alpha) = \frac{\overline{V}_m}{\overline{W}}$$

and these equations yield

$$m' = \frac{x_b' \overline{V}_m}{\overline{W}} - \frac{y_b' (\overline{V}_\theta + r'\Omega)}{\overline{W}}$$

and

$$\theta' = \frac{x_b' (\overline{V}_\theta + r'\Omega)}{r'\overline{W}} + \frac{y_b' \overline{V}_m}{r'\overline{W}} .$$

From the velocity diagram of Figure 7, we get

$$-\frac{\overline{V}_\theta}{\overline{V}_m} = \tan(\beta) .$$

We can now rewrite the last two terms in the last exponential of the expression for the distortion velocity,

$$
\begin{aligned}
-n\theta' + \frac{n\,m'\overline{V}_\theta}{r'\overline{V}_m} &= -\frac{n\,x_b'(\overline{V}_\theta + r'\Omega)}{r'\overline{W}} - \frac{n\,y_b'\overline{V}_m}{r'\overline{W}} + \frac{n\,x_b'\overline{V}_\theta}{r'\overline{W}} \\
&\quad - \frac{n\,y_b'\overline{V}_\theta\,(\overline{V}_\theta + r'\Omega)}{r'\overline{V}_m\overline{W}} \\
&= -\frac{n\Omega x_b'}{\overline{W}} - \frac{n\Omega y_b'}{\overline{W}}\left[\frac{\overline{V}_\theta\,(\overline{V}_\theta + r'\Omega) + \overline{V}_m\overline{V}_m}{r'\Omega\overline{V}_m}\right] \\
&= -\frac{n\Omega x_b'}{\overline{W}} - \frac{n\Omega y_b'}{\overline{W}}\left[\frac{\overline{V}_m\overline{V}_m + \overline{V}_\theta\,(\overline{V}_\theta + r'\Omega)}{-\overline{V}_m\overline{V}_\theta + r'\Omega\overline{V}_m + \overline{V}_m\overline{V}_\theta}\right] \\
&= -\frac{n\Omega x_b'}{\overline{W}} - \frac{n\Omega y_b'}{\overline{W}}\left[\frac{1 + \left(\frac{\overline{V}_\theta}{\overline{V}_m}\right)\left(\frac{\overline{V}_\theta + r'\Omega}{\overline{V}_m}\right)}{-\left(\frac{\overline{V}_\theta}{\overline{V}_m}\right) + \left(\frac{\overline{V}_\theta + r'\Omega}{\overline{V}_m}\right)}\right] \\
&= -\frac{n\Omega x_b'}{\overline{W}} - \frac{n\Omega y_b'}{\overline{W}}\left[\frac{1 - \tan(\beta)\tan(\gamma+\alpha)}{\tan(\beta) + \tan(\gamma+\alpha)}\right] \\
&= -\frac{n\Omega x_b'}{\overline{W}} - \frac{n\Omega y_b'}{\overline{W}}\cot(\beta+\gamma+\alpha) \\
&= -\frac{n\Omega x_b'}{\overline{W}} + \left(\frac{\widetilde{u}}{\widetilde{v}}\right)\frac{n\Omega y_b'}{\overline{W}}\,.
\end{aligned}
$$

We now obtain

$$
\begin{aligned}
\widetilde{V}_n(x_b', y_b', r', t, \ell) &= |\widetilde{V}_n|\, e^{-\delta_n(m' + z_{r_{mc}})/\overline{V}_m} \\
&\quad e^{i\left[n\Omega t - \frac{n\,2\pi\ell}{B} + \phi_n - n\psi_{mc} + \frac{n z_{r_{mc}}\overline{V}_\theta}{r'\overline{V}_m} - \frac{n\Omega x_b'}{\overline{W}} + \left(\frac{\widetilde{u}}{\widetilde{v}}\right)\frac{n\Omega y_b'}{\overline{W}}\right]}\,.
\end{aligned}
$$

The calculations of the unsteady lift in the (x_b', y_b', r') coordinate system requires us to resolve the distortion velocity into components in the x_b' direction, $\widetilde{u}$, and the y_b' direction, $\widetilde{v}$. We can compute these components as follows

$$
\begin{aligned}
\widetilde{u}_n(x_b', y_b', r', t, \ell) &= \widetilde{V}_n\cos(\beta+\gamma+\alpha) \\
&= \widetilde{V}_n\cos(\beta)\cos(\gamma+\alpha) - \widetilde{V}_n\sin(\beta)\sin(\gamma+\alpha) \\
&= \widetilde{V}_{m_n}\cos(\gamma+\alpha) + \widetilde{V}_{\theta_n}\sin(\gamma+\alpha)
\end{aligned}
$$

and

$$
\begin{aligned}
\widetilde{v}_n(x_b', y_b', r', t, \ell) &= -\widetilde{V}_n\sin(\beta+\gamma+\alpha) \\
&= -\widetilde{V}_n\sin(\beta)\cos(\gamma+\alpha) - \widetilde{V}_n\cos(\beta)\sin(\gamma+\alpha) \\
&= -\widetilde{V}_{m_n}\sin(\gamma+\alpha) + \widetilde{V}_{\theta_n}\cos(\gamma+\alpha)\,.
\end{aligned}
$$

In this section, we will use the equation for the unsteady lift per unit span on an isolated airfoil derived by Naumann and Yeh [1973],

$$\widetilde{L}_n \;=\; \frac{1}{2}\frac{dC_L}{d\alpha}\rho c\overline{W}\left[\widetilde{v}_n\, S(\omega_n) \;+\; \alpha\widetilde{u}_n\, F_\alpha(\omega_n) \;+\; \frac{2y_m\widetilde{u}_n}{c}\, F_f(\omega_n)\right] .$$

The expressions for $\widetilde{u}$ and $\widetilde{v}$ were used in the derivation of this equation. The term involving y_b' dropped out since we are only interested in the effects on the blade surface where $y_b' = 0$ in the thin airfoil approximations. The term involving x_b' became part of three larger expressions in deriving the functions S, F_α, and F_f. These expressions were integrated from $x_b' = -\frac{c}{2}$ to $x_b' = \frac{c}{2}$. For the chord, we should estimate the projection of the chord in the meridional direction. This allows us to use a two-dimensional method along a circumferential-mean streamsurface where three-dimensional flow effects should be minimized. The values of $\frac{dC_L}{d\alpha}$, c, $\overline{W}$, α, and y_m are all a function of the radius.

Before computing the total unsteady force components due to all blades, all radial sections, and all inflow harmonics, we must decide where the unsteady lift acts on each blade section. In his analysis, Sears [1941] calculated that the unsteady lift would act at $x_b' = -\frac{c}{4}$. We must calculate the unsteady lift at the location in which it acts in order to avoid calculating the corresponding unsteady moments along the chord. For small values of α, the relationship between the midchord skew and rake and the skew and rake at x_{b_o}' is

$$\psi_{mc} \;\approx\; \psi \;-\; \frac{x_{b_o}'}{r'}\sin(\gamma)$$

and

$$z_{mc} \;\approx\; z_r \;-\; x_{b_o}'\cos(\gamma) .$$

We can now rewrite the skew and rake terms of the distortion velocity exponential as

$$\begin{aligned} -n\psi_{mc} \;+\; \frac{nz_{r_{mc}}\overline{V}_\theta}{r'\overline{V}_m} \;&\approx\; -n\psi \;+\; \frac{nx_{b_o}'}{r'}\sin(\gamma) \;+\; \frac{nz_r\overline{V}_\theta}{r'\overline{V}_m} \;-\; \frac{nx_{b_o}'\overline{V}_\theta}{r'\overline{V}_m}\cos(\gamma) \\ &\approx\; -n\psi \;+\; \frac{nz_r\overline{V}_\theta}{r'\overline{V}_m} \\ &\quad +\; \frac{n\Omega x_{b_o}'}{\overline{W}}\left[\frac{\overline{W}}{r'\Omega}\sin(\gamma) \;-\; \frac{\overline{W}\,\overline{V}_\theta}{r'\Omega\overline{V}_m}\cos(\gamma)\right] . \end{aligned}$$

Using Figure 7 and the law of sines gives

$$\frac{\overline{W}}{r'\Omega} = \frac{\sin(\frac{\pi}{2} - \beta)}{\sin(\beta + \gamma + \alpha)} = \frac{\cos(\beta)}{\sin(\beta + \gamma + \alpha)} .$$

The unsteady thin airfoil theory that we use to compute the unsteady lift assumes a small value of α. Using a small angle approximation gives

$$\sin(\beta + \gamma + \alpha) \approx \sin(\beta + \gamma) = \sin(\beta)\cos(\gamma) + \cos(\beta)\sin(\gamma) .$$

From the velocity diagram of Figure 7, we get

$$-\frac{\overline{V}_\theta}{\overline{V}_m} = \tan(\beta)$$

and finally

$$\begin{aligned} -n\psi_{mc} + \frac{nz_{r_{mc}}\overline{V}_\theta}{r'\overline{V}_m} &\approx -n\psi + \frac{nz_r\overline{V}_\theta}{r'\overline{V}_m} \\ &\quad + \frac{n\Omega x'_{b_o}}{\overline{W}} \left\{ \frac{\cos(\beta)\sin(\gamma)}{\sin(\beta)\cos(\gamma) + \cos(\beta)\sin(\gamma)} \right. \\ &\quad \left. - \left[\frac{-\sin(\beta)}{\cos(\beta)}\right] \frac{\cos(\beta)\cos(\gamma)}{\sin(\beta)\cos(\gamma) + \cos(\beta)\sin(\gamma)} \right\} \\ &\approx -n\psi + \frac{nz_r\overline{V}_\theta}{r'\overline{V}_m} + \frac{n\Omega x'_{b_o}}{\overline{W}} . \end{aligned}$$

This equation yields two methods to compute the unsteady lift at the quarter chord. We can move the coordinate system from (x'_b, y'_b, r') to $(x'_b - \frac{c}{4}, y'_b, r')$ and simply use the values of skew and rake at this new location. Or we can compute the unsteady lift at midchord and then move the location of the unsteady lift to the quarter chord by multiplying by $e^{-in\Omega c/4\overline{W}}$. The dependence of the location of the coordinate system in computing unsteady lift can be demonstrated by the lift function developed by Brown [1964] as seen in Figure 8. For a particular reduced frequency, the amplitude of unsteady lift does not change with coordinate system location. Only the phase angle of the unsteady lift is affected. We can compute the change in unsteady lift by

$$\widetilde{L}_{n,x'_{b_o}} = \widetilde{L}_{n,mc}\, e^{in\Omega x'_{b_o}/\overline{W}} .$$

Since we must eventually sum the unsteady forces radially, we should compute the unsteady lift at the location where the unsteady lift acts. This new rotating coordinate system is shown in Figure 9 and the transformation from the stationary coordinate system to this new rotating coordinate system would have used the skew and the rake at quarter chord instead of at midchord. Therefore, to obtain the unsteady lift acting at quarter chord, we use the following expression for the distortion velocity prior to using the equation for the unsteady lift:

$$\widetilde{V}_n(x'_b, y'_b, r', t, \ell) = |\widetilde{V}_n| e^{-\delta_n(m' + z_r)/\overline{V}_m} e^{i\left[n\Omega t - \frac{n2\pi\ell}{B} + \phi_n - n\psi + \frac{nz_r\overline{V}_\theta}{r'\overline{V}_m} - \frac{n\Omega x'_h}{\overline{W}} + \left(\frac{s}{t}\right)\frac{n\Omega y'_h}{\overline{W}}\right]} .$$

After adjusting the measured inflow phase angle for skew and rake at quarter chord, we compute an unsteady lift for each blade,

$$\widetilde{L}_n(r', t, \ell) = |\widetilde{L}_n| e^{i\left(n\Omega t - \frac{n2\pi\ell}{B} + \Phi_n\right)} .$$

This unsteady lift acts in the positive y'_b direction (see Figure 9). Now we can determine the components of this unsteady lift in the z', r', and θ' directions as

$$\widetilde{F}_{z'_n}(r', t, \ell) = -\widetilde{L}_n \sin(\gamma + \alpha) \cos(\mu) ,$$

$$\widetilde{F}_{r'_n}(r', t, \ell) = -\widetilde{L}_n \sin(\gamma + \alpha) \sin(\mu) ,$$

and

$$\widetilde{F}_{\theta'_n}(r', t, \ell) = \widetilde{L}_n \cos(\gamma + \alpha)$$

where

$$\mu = \tan^{-1}\left(\frac{\overline{V}_r}{\overline{V}_z}\right) .$$

μ represents the inclination of the streamlines to the axial direction. To calculate the total unsteady force acting on the shaft in the z' direction, we must move all of the $\widetilde{F}_{z'_n}$ vectors to a point on the shaft centerline. This involves summing the $\widetilde{F}_{z'_n}$ vectors over all inflow harmonics, all blades, and all radial sections,

$$\widetilde{F}_{z'}(t) = -\sum_{r'=r_H}^{r_T} \sum_{\ell=1}^{B} \sum_{n=1}^{\infty} |\widetilde{L}_n| \sin(\gamma + \alpha) \cos(\mu) e^{i\left(n\Omega t - \frac{n2\pi\ell}{B} + \Phi_n\right)} .$$

From the summation relationships of Gradshteyn and Ryzhik [1980], we can easily derive

$$\sum_{\ell=1}^{B} e^{-in2\pi\ell/B} = \begin{cases} B & \text{if } n = kB \\ 0 & \text{if } n \neq kB \end{cases} .$$

Using this relationship allows us to obtain

$$\widetilde{F}_{z'}(t) = -B \sum_{r'=r_H}^{r_T} \sum_{k=1}^{\infty} |\widetilde{L}_{kB}| \sin(\gamma+\alpha) \cos(\mu) e^{i(kB\Omega t + \Phi_{kB})} .$$

This force is the negative of the unsteady thrust on the shaft. The unsteady thrust occurs at frequencies that are integer multiples of the blade passing frequency and can be computed from the inflow harmonics corresponding to these frequencies. We denote the multiples of blade rate harmonics with the subscript k.

We can also calculate the unsteady side forces on the shaft. The components of unsteady force in the r' and θ' directions must be resolved into components of unsteady force in the x' and y' directions. Using Figure 10, we calculate the total unsteady force in the x' direction,

$$\begin{aligned} \widetilde{F}_{x'}(t) = & \sum_{r'=r_H}^{r_T} \sum_{\ell=1}^{B} \sum_{n=1}^{\infty} |\widetilde{L}_n| \sin(\gamma+\alpha) \sin(\mu) \cos\left(\psi - \frac{2\pi\ell}{B} - \frac{\pi}{2}\right) \\ & e^{i\left(n\Omega t - \frac{n2\pi\ell}{B} + \Phi_n\right)} \\ & - \sum_{r'=r_H}^{r_T} \sum_{\ell=1}^{B} \sum_{n=1}^{\infty} |\widetilde{L}_n| \cos(\gamma+\alpha) \cos\left(\psi - \frac{2\pi\ell}{B}\right) \\ & e^{i\left(n\Omega t - \frac{n2\pi\ell}{B} + \Phi_n\right)} . \end{aligned}$$

We can write the last cosine factor in each term as a sum of exponentials using Euler's Formula,

$$\begin{aligned}
\widetilde{F}_{x'}(t) \;=\; & \frac{1}{2}\sum_{r'=r_H}^{r_T}\sum_{\ell=1}^{B}\sum_{n=1}^{\infty}|\widetilde{L}_n|\sin(\gamma+\alpha)\,\sin(\mu) \\
& \qquad e^{i\left[n\Omega t\,-\,(n+1)\frac{2\pi\ell}{B}\,+\,\Phi_n\,+\,\psi\,-\,\frac{\pi}{2}\right]} \\
& + \frac{1}{2}\sum_{r'=r_H}^{r_T}\sum_{\ell=1}^{B}\sum_{n=1}^{\infty}|\widetilde{L}_n|\sin(\gamma+\alpha)\,\sin(\mu) \\
& \qquad e^{i\left[n\Omega t\,-\,(n-1)\frac{2\pi\ell}{B}\,+\,\Phi_n\,-\,\psi\,+\,\frac{\pi}{2}\right]} \\
& - \frac{1}{2}\sum_{r'=r_H}^{r_T}\sum_{\ell=1}^{B}\sum_{n=1}^{\infty}|\widetilde{L}_n|\cos(\gamma+\alpha) \\
& \qquad e^{i\left[n\Omega t\,-\,(n+1)\frac{2\pi\ell}{B}\,+\,\Phi_n\,+\,\psi\right]} \\
& - \frac{1}{2}\sum_{r'=r_H}^{r_T}\sum_{\ell=1}^{B}\sum_{n=1}^{\infty}|\widetilde{L}_n|\cos(\gamma+\alpha) \\
& \qquad e^{i\left[n\Omega t\,-\,(n-1)\frac{2\pi\ell}{B}\,+\,\Phi_n\,-\,\psi\right]}\,.
\end{aligned}$$

The summation relations of Gradshteyn and Ryzhik [1980] yield

$$\sum_{\ell=1}^{B} e^{-i(n\pm1)2\pi\ell/B} \;=\; \begin{cases} B & \text{if} \quad (n\pm1) \;=\; kB \\ 0 & \text{if} \quad (n\pm1) \;\neq\; kB \end{cases}.$$

We can now write

$$\begin{aligned}
\widetilde{F}_{x'}(t) \;=\; & \frac{B}{2}\sum_{r'=r_H}^{r_T}\sum_{k=1}^{\infty}|\widetilde{L}_{kB-1}|\left[\sin(\gamma+\alpha)\,\sin(\mu)\,e^{-i\pi/2}\;-\;\cos(\gamma+\alpha)\right] \\
& \qquad e^{i[(kB-1)\Omega t\,+\,\Phi_{kB-1}\,+\,\psi]} \\
& + \frac{B}{2}\sum_{r'=r_H}^{r_T}\sum_{k=1}^{\infty}|\widetilde{L}_{kB+1}|\left[\sin(\gamma+\alpha)\,\sin(\mu)\,e^{i\pi/2}\;-\;\cos(\gamma+\alpha)\right] \\
& \qquad e^{i[(kB+1)\Omega t\,+\,\Phi_{kB+1}\,-\,\psi]}\,.
\end{aligned}$$

We can compute the total unsteady force in the y' direction in the same manner:

$$\begin{aligned}
\widetilde{F}_{y'}(t) \;=\; & \frac{B}{2}\sum_{r'=r_H}^{r_T}\sum_{k=1}^{\infty}|\widetilde{L}_{kB-1}|\left[-\sin(\gamma+\alpha)\,\sin(\mu)\;-\;\cos(\gamma+\alpha)\,e^{-i\pi/2}\right] \\
& \qquad e^{i[(kB-1)\Omega t\,+\,\Phi_{kB-1}\,+\,\psi]} \\
& + \frac{B}{2}\sum_{r'=r_H}^{r_T}\sum_{k=1}^{\infty}|\widetilde{L}_{kB+1}|\left[-\sin(\gamma+\alpha)\,\sin(\mu)\;-\;\cos(\gamma+\alpha)\,e^{i\pi/2}\right] \\
& \qquad e^{i[(kB+1)\Omega t\,+\,\Phi_{kB+1}\,-\,\psi]}\,.
\end{aligned}$$

In order to better compare $\widetilde{F}_{y'}$ with $\widetilde{F}_{x'}$, we can also write $\widetilde{F}_{y'}$ as

$$\widetilde{F}_{y'}(t) = \frac{B}{2} \sum_{r'=r_H}^{r_T} \sum_{k=1}^{\infty} |\widetilde{L}_{kB-1}| \left[\sin(\gamma+\alpha) \sin(\mu) e^{-i\pi/2} - \cos(\gamma+\alpha) \right] e^{i\left[(kB-1)\Omega t + \Phi_{kB-1} + \psi - \frac{\pi}{2}\right]}$$

$$+ \frac{B}{2} \sum_{r'=r_H}^{r_T} \sum_{k=1}^{\infty} |\widetilde{L}_{kB+1}| \left[\sin(\gamma+\alpha) \sin(\mu) e^{i\pi/2} - \cos(\gamma+\alpha) \right] e^{i\left[(kB+1)\Omega t + \Phi_{kB+1} - \psi + \frac{\pi}{2}\right]} .$$

In the rotating coordinate system, the unsteady side forces occur at frequencies adjacent to the integer multiples of blade passing frequency and are computed from inflow harmonics corresponding to these frequencies. A 90 degree phase shift exists between the portions of unsteady side force in the x' and y' directions that occur at each of the adjacent frequencies.

The unsteady forces on the blades also create unsteady moments at the point on the shaft centerline where we computed the unsteady forces. Vectorially, we can compute the unsteady moment at this point by

$$\overrightarrow{\widetilde{M}}(r',t,\ell) = \left(\overrightarrow{r'} + \overrightarrow{z_r} \right) \times \overrightarrow{\widetilde{L}_n}(r',t,\ell) .$$

The components of this unsteady moment in the z', r', and θ' directions are

$$\widetilde{M}_{z'_n}(r',t,\ell) = r' \widetilde{F}_{\theta'_n}$$

$$= r' \widetilde{L}_n \cos(\gamma+\alpha) ,$$

$$\widetilde{M}_{r'_n}(r',t,\ell) = -z_r \widetilde{F}_{\theta'_n}$$

$$= -z_r \widetilde{L}_n \cos(\gamma+\alpha) ,$$

and

$$\widetilde{M}_{\theta'_n}(r',t,\ell) = -r' \widetilde{F}_{z'_n} + z_r \widetilde{F}_{r'_n}$$

$$= r' \widetilde{L}_n \sin(\gamma+\alpha) \cos(\mu) - z_r \widetilde{L}_n \sin(\gamma+\alpha) \sin(\mu) .$$

We can compute the components of the total unsteady moment in the z', x', and y' direction in the same manner as the unsteady force components:

$$\widetilde{M}_{z'}(t) = B \sum_{r'=r_H}^{r_T} \sum_{k=1}^{\infty} |\widetilde{L}_{kB}| r' \cos(\gamma+\alpha) e^{i(kB\Omega t + \Phi_{kB})} ,$$

$$\widetilde{M}_{x'}(t) = \frac{B}{2} \sum_{r'=r_H}^{r_T} \sum_{k=1}^{\infty} |\widetilde{L}_{kB-1}| \Big[z_r \cos(\gamma+\alpha)\, e^{-i\pi/2} - r' \sin(\gamma+\alpha) \cos(\mu) + z_r \sin(\gamma+\alpha) \sin(\mu) \Big] e^{i[(kB-1)\Omega t + \Phi_{kB-1} + \psi]}$$

$$+ \frac{B}{2} \sum_{r'=r_H}^{r_T} \sum_{k=1}^{\infty} |\widetilde{L}_{kB+1}| \Big[z_r \cos(\gamma+\alpha)\, e^{i\pi/2} - r' \sin(\gamma+\alpha) \cos(\mu) + z_r \sin(\gamma+\alpha) \sin(\mu) \Big] e^{i[(kB+1)\Omega t + \Phi_{kB+1} - \psi]} ,$$

and

$$\widetilde{M}_{y'}(t) = \frac{B}{2} \sum_{r'=r_H}^{r_T} \sum_{k=1}^{\infty} |\widetilde{L}_{kB-1}| \Big[z_r \cos(\gamma+\alpha)\, e^{-i\pi/2} - r' \sin(\gamma+\alpha) \cos(\mu) + z_r \sin(\gamma+\alpha) \sin(\mu) \Big] e^{i\left[(kB-1)\Omega t + \Phi_{kB-1} + \psi - \frac{\pi}{2}\right]}$$

$$+ \frac{B}{2} \sum_{r'=r_H}^{r_T} \sum_{k=1}^{\infty} |\widetilde{L}_{kB+1}| \Big[z_r \cos(\gamma+\alpha)\, e^{i\pi/2} - r' \sin(\gamma+\alpha) \cos(\mu) + z_r \sin(\gamma+\alpha) \sin(\mu) \Big] e^{i\left[(kB+1)\Omega t + \Phi_{kB+1} - \psi + \frac{\pi}{2}\right]} .$$

The unsteady torque, $-\widetilde{M}_{z'}$, occurs at integer multiples of the blade passing frequency while the unsteady bending moments occur at the frequencies adjacent to the integer multiples of the blade passing frequency.

We have now computed the various components of unsteady force and unsteady moment on the rotor shaft for a coordinate system rotating with the shaft. Next, we need to transform these forces and moments to a stationary coordinate system as shown in Figure 11. The z components of the unsteady force and moment are exactly the same as the z' components:

$$\widetilde{F}_z(t) = -B \sum_{r=r_H}^{r_T} \sum_{k=1}^{\infty} |\widetilde{L}_{kB}| \sin(\gamma+\alpha) \cos(\mu)\, e^{i(kB\Omega t + \Phi_{kB})}$$

and

$$\widetilde{M}_z(t) = B \sum_{r=r_H}^{r_T} \sum_{k=1}^{\infty} |\widetilde{L}_{kB}| r \cos(\gamma+\alpha)\, e^{i(kB\Omega t + \Phi_{kB})} .$$

Using Figure 12, we can write the relation between the two coordinate systems as

$$x = x' \cos(-\Omega t) + y' \sin(-\Omega t)$$

and

$$y = -x' \sin(-\Omega t) + y' \cos(-\Omega t) .$$

The transformations for unsteady side forces are

$$\begin{aligned}\widetilde{F}_x(t) &= \widetilde{F}_{x'}\cos(-\Omega t) + \widetilde{F}_{y'}\cos\left(-\Omega t - \frac{\pi}{2}\right)\\ &= \widetilde{F}_{x'}\cos(\Omega t) + \widetilde{F}_{y'}\cos\left(\Omega t + \frac{\pi}{2}\right)\end{aligned}$$

and

$$\begin{aligned}\widetilde{F}_y(t) &= -\widetilde{F}_{x'}\cos\left(-\Omega t - \frac{\pi}{2}\right) + \widetilde{F}_{y'}\cos(-\Omega t)\\ &= -\widetilde{F}_{x'}\cos\left(\Omega t + \frac{\pi}{2}\right) + \widetilde{F}_{y'}\cos(\Omega t)\ .\end{aligned}$$

We can change these transformations to exponentials using Euler's Formula:

$$\widetilde{F}_x(t) = \frac{1}{2}\left[\widetilde{F}_{x'}e^{i\Omega t} + \widetilde{F}_{x'}e^{-i\Omega t} + \widetilde{F}_{y'}e^{i(\Omega t + \frac{\pi}{2})} + \widetilde{F}_{y'}e^{-i(\Omega t + \frac{\pi}{2})}\right]$$

and

$$\widetilde{F}_y(t) = \frac{1}{2}\left[-\widetilde{F}_{x'}e^{i(\Omega t + \frac{\pi}{2})} - \widetilde{F}_{x'}e^{-i(\Omega t + \frac{\pi}{2})} + \widetilde{F}_{y'}e^{i\Omega t} + \widetilde{F}_{y'}e^{-i\Omega t}\right]\ .$$

We can now compute the unsteady horizontal side force in the stationary coordinate system:

$$\begin{aligned}\widetilde{F}_x(t) = {} & \frac{B}{4}\sum_{r=r_H}^{r_T}\sum_{k=1}^{\infty}|\widetilde{L}_{kB-1}|\\ & \Big\{\left[\sin(\gamma+\alpha)\sin(\mu)e^{-i\pi/2} - \cos(\gamma+\alpha)\right]e^{ikB\Omega t}\\ & + \left[\sin(\gamma+\alpha)\sin(\mu)e^{-i\pi/2} - \cos(\gamma+\alpha)\right]e^{i(kB-2)\Omega t}\\ & + \left[\sin(\gamma+\alpha)\sin(\mu)e^{-i\pi/2} - \cos(\gamma+\alpha)\right]e^{ikB\Omega t}\\ & + \left[-\sin(\gamma+\alpha)\sin(\mu)e^{-i\pi/2} + \cos(\gamma+\alpha)\right]e^{i(kB-2)\Omega t}\Big\}\\ & e^{i(\Phi_{kB-1}+\psi)}\\ & + \frac{B}{4}\sum_{r=r_H}^{r_T}\sum_{k=1}^{\infty}|\widetilde{L}_{kB+1}|\\ & \Big\{\left[\sin(\gamma+\alpha)\sin(\mu)e^{i\pi/2} - \cos(\gamma+\alpha)\right]e^{i(kB+2)\Omega t}\\ & + \left[\sin(\gamma+\alpha)\sin(\mu)e^{i\pi/2} - \cos(\gamma+\alpha)\right]e^{ikB\Omega t}\\ & + \left[-\sin(\gamma+\alpha)\sin(\mu)e^{i\pi/2} + \cos(\gamma+\alpha)\right]e^{i(kB+2)\Omega t}\\ & + \left[\sin(\gamma+\alpha)\sin(\mu)e^{i\pi/2} - \cos(\gamma+\alpha)\right]e^{ikB\Omega t}\Big\}\\ & e^{i(\Phi_{kB+1}-\psi)}\ .\end{aligned}$$

This expression simplifies to

$$\widetilde{F}_x(t) = \frac{B}{2}\sum_{r=r_H}^{r_T}\sum_{k=1}^{\infty}|\widetilde{L}_{kB-1}|\left[\sin(\gamma+\alpha)\sin(\mu)\,e^{-i\pi/2} - \cos(\gamma+\alpha)\right] e^{i(kB\Omega t + \Phi_{kB-1} + \psi)} + \frac{B}{2}\sum_{r=r_H}^{r_T}\sum_{k=1}^{\infty}|\widetilde{L}_{kB+1}|\left[\sin(\gamma+\alpha)\sin(\mu)\,e^{i\pi/2} - \cos(\gamma+\alpha)\right] e^{i(kB\Omega t + \Phi_{kB+1} - \psi)} .$$

We can formulate the expressions for $\widetilde{F}_y$, $\widetilde{M}_x$, and $\widetilde{M}_y$ in the same manner:

$$\widetilde{F}_y(t) = \frac{B}{2}\sum_{r=r_H}^{r_T}\sum_{k=1}^{\infty}|\widetilde{L}_{kB-1}|\left[\sin(\gamma+\alpha)\sin(\mu)\,e^{-i\pi/2} - \cos(\gamma+\alpha)\right] e^{i\left(kB\Omega t + \Phi_{kB-1} + \psi - \frac{\pi}{2}\right)} + \frac{B}{2}\sum_{r=r_H}^{r_T}\sum_{k=1}^{\infty}|\widetilde{L}_{kB+1}|\left[\sin(\gamma+\alpha)\sin(\mu)\,e^{i\pi/2} - \cos(\gamma+\alpha)\right] e^{i\left(kB\Omega t + \Phi_{kB+1} - \psi + \frac{\pi}{2}\right)} ,$$

$$\widetilde{M}_x(t) = \frac{B}{2}\sum_{r=r_H}^{r_T}\sum_{k=1}^{\infty}|\widetilde{L}_{kB-1}|\left[z_r\cos(\gamma+\alpha)\,e^{-i\pi/2} - r\sin(\gamma+\alpha)\cos(\mu) + z_r\sin(\gamma+\alpha)\sin(\mu)\right] e^{i(kB\Omega t + \Phi_{kB-1} + \psi)} + \frac{B}{2}\sum_{r=r_H}^{r_T}\sum_{k=1}^{\infty}|\widetilde{L}_{kB+1}|\left[z_r\cos(\gamma+\alpha)\,e^{i\pi/2} - r\sin(\gamma+\alpha)\cos(\mu) + z_r\sin(\gamma+\alpha)\sin(\mu)\right] e^{i(kB\Omega t + \Phi_{kB+1} - \psi)} ,$$

and

$$\widetilde{M}_y(t) = \frac{B}{2}\sum_{r=r_H}^{r_T}\sum_{k=1}^{\infty}|\widetilde{L}_{kB-1}|\left[z_r\cos(\gamma+\alpha)\,e^{-i\pi/2} - r\sin(\gamma+\alpha)\cos(\mu) + z_r\sin(\gamma+\alpha)\sin(\mu)\right] e^{i\left(kB\Omega t + \Phi_{kB-1} + \psi - \frac{\pi}{2}\right)} + \frac{B}{2}\sum_{r=r_H}^{r_T}\sum_{k=1}^{\infty}|\widetilde{L}_{kB+1}|\left[z_r\cos(\gamma+\alpha)\,e^{i\pi/2} - r\sin(\gamma+\alpha)\cos(\mu) + z_r\sin(\gamma+\alpha)\sin(\mu)\right] e^{i\left(kB\Omega t + \Phi_{kB+1} - \psi + \frac{\pi}{2}\right)} .$$

The unsteady side forces and bending moments are exactly the same in the rotating and stationary coordinate systems except that they occur at frequencies adjacent to the integer multiples of blade passing frequency in the rotating coordinate system and they occur at the integer multiples of blade passing frequency in the stationary coordinate system.

Conclusions

We have presented a method for computing the unsteady forces and moments on the shaft of a rotor blade row operating within a nonuniform inflow. The method uses a Fourier analysis and several coordinate transformations to develop equations for all six components of unsteady forces and moments–in both a stationary coordinate system and a coordinate system rotating with the rotor shaft. This strip theory does incorporate the rake and skew of the rotor blades. In the stationary coordinate system, all of the components of the unsteady forces and moments occur at integer multiples of the blade passing frequency. The unsteady thrust and torque are computed from the inflow harmonics corresponding to these frequencies while the unsteady side forces and bending moments are computed from the inflow harmonics corresponding to frequencies adjacent to the integer multiples of blade passing frequency. The only difference in these results when we switch to a coordinate system rotating with the blades is that the unsteady side forces and bending moments actually occur at frequencies adjacent to the integer multiples of blade passing frequency.

This two-dimensional strip theory can be used in conjunction with any two-dimensional method for computing the unsteady lift on a single rotor blade operating within a nonuniform inflow. If we use an unsteady thin airfoil technique, the method proves to be very fast and adequate for predicting trends. A computer program has been written using the unsteady thin airfoil theory of Naumann and Yeh [1973] with options to use the methods of Weinig [1935] and Whitehead [1960]. This Penn State ARL code uses Fourier analyzed wake surveys measured at several radii. Because of the finite number of radial and circumferential measurements as well as the many approximations involved in the unsteady thin airfoil technique, we should not depend on these calculations to obtain absolute unsteady force levels. However, comparing

calculations using different blade designs gives important trends of how the different designs affect the unsteady forces and moments. Hopefully, engineers will incorporate these and other unsteady force computations within the turbomachinery design process.

Bibliography

Atassi, H. M., "The Sears Problem for a Lifting Airfoil Revisited–New Results," *Journal of Fluid Mechanics*, Vol. 141, pp 109–122, 1984.

Brown, N. A., "Periodic Propeller Forces in Non-Uniform Flow," MIT Report No. 64-7, 1964.

Dean, R. C., "On the Necessity of Unsteady Flow in Fluid Mechanics," Transactions of ASME, *Journal of Basic Engineering*, pp. 24–28, March 1959.

Evans, B. J., "Effects of Free-stream Turbulence on Blade Performance in a Compressor Cascade," Ph. D. Dissertation, Cambridge University, 1978.

Fleeter, S., "Fluctuating Lift and Moment Coefficients for Cascaded Airfoils in a Nonuniform Compressible Flow," *AIAA Journal of Aircraft*, Vol. 10, No. 2, February 1973.

Gradshteyn, I. S. and Ryzhik, I. M., *Table of Integrals, Series, and Products*, Translated and Edited by A. Jeffery, Academic Press, 1980.

Goldstein, M. E. and Atassi, H. M., "A Complete Second-order Theory for the Unsteady Flow about as Airfoil Due to a Periodic Gust," *Journal of Fluid Mechanics*, Vol. 74, Part 4, pp. 741–765, 1976.

Henderson, R. E., "Unsteady Response of an Axial Flow Turbomachine to an Upstream Disturbance," Ph. D. Thesis, Cambridge University, 1972.

Hodson, H. P., "The Development of Unsteady Boundary Layers on the Rotor of an Axial-Flow Turbomachine," AGARD-CP-351, June 1983.

Hodson, H. P., "An Inviscid Blade-to-Blade Prediction of a Wake-Generated Unsteady Flow," Transactions of ASME, *Journal of Engineering for Gas Turbines and Power*, Vol. 107, April 1985.

Horlock, J. H., "Fluctuating Lift Forces on Aerofoils Moving Through Transverse and Chordwise Gusts," Transactions of ASME, *Journal of Basic Engineering*, Vol. 90D, No. 4, pp. 494–500, 1968a.

Horlock, J. H., "Unsteady Flow in Turbomachines," Presented at the Third Australian Conference on Hydraulics and Fluid Mechanics, Sidney, Australia, November 1968b.

Kemp, N. H. and Sears, W. R., "Aerodynamic Interference Between Moving Blade Rows," *Journal of the Aeronautical Sciences*, Vol. 20, pp. 585–598, 1953.

Kerrebrock, J. L. and Mikolajczak, A. A., "Intra-Stator Transport of Rotor Wakes and its Effect on Compressor Performance," Transactions of ASME, *Journal of Engineering for Power*, pp. 359–368, October 1970.

Kerwin, J. E. and Lee, C. S., "Prediction of Steady and Unsteady Marine Propeller Performance by Numerical Lifting Surface Theory," *Transactions of SNAME*, Vol. 86, pp. 218–253, 1978.

Koya, M. and Kotake, S., "Numerical Analysis of Fully Three-Dimensional Flows through a Turbine Stage," Transactions of the ASME, *Journal of Engineering for Gas Turbines and Power*, Vol. 107, pp. 945–952, October 1985.

Lefcort, M. P., "An Investigation into Unsteady Blade Forces in Turbomachines," Transactions of ASME, *Journal of Engineering for Power*, October 1965.

Lienhart, W., "Berechnung der instationären Srömung durch gegeneinander bewegte Schaufelgitter und der Schaufelkraftschwankungen," VDI-Forschungsheft 562, Düsseldorf, 1974.

Meyer, R. X., "The Effect of Wakes on the Transient Pressure and Velocity Distributions in Turbomachines," Transactions of ASME, Vol. 80, pp. 1544–1552, 1958.

Naumann, H. and Yeh, H., "Lift and Pressure Fluctuations of a Cambered Airfoil Under Periodic Gusts and Applications in Turbomachinery," Transactions of ASME, *Journal of Engineering for Power*, Series A, Vol. 95, No. 1, 1973.

Osborne, C., "Unsteady Thin-Airfoil Theory for Subsonic Flow," *AIAA Journal*, Vol. 11, No. 2, pp. 205–209, 1973.

Sears, W. R., "Some Aspects of Non-Stationary Airfoil Theory," *Journal of Aeronautical Sciences*, Vol. 8, pp. 104–108, 1941.

Smith, S. N., "Discrete Frequency Sound Generation in Axial Flow Turbomachines," University of Cambridge, Department of Engineering Rep. No. CUED/A-TURBO/TR29, 1971.

Strouhal, V., "Über eine besondere Art der Tonerregung," *Ann. Phys. und Chemie*, New Series 5, pp. 216–251, 1878.

Theodorsen, T., "General Theory of Aerodynamic Instability and the Mechanism of Flutter," NACA Technical Report No. 496, 1935.

Tsakonas, S., Jacobs, W. R., and Ali, M. R., "An Exact Linear Lifting Surface Theory for Marine Propeller in a Nonuniform Flow Field," *Journal of Ship Research*, Vol. 17, No. 4, pp. 196–207, 1973.

Tsakonas, S., Jacobs, W. R., and Liao, P., "Blade Pressure Distribution for a Moderately Loaded Propeller," *Journal of Ship Research*, Vol. 27, No. 1, pp. 39–55, 1983.

Von Kármán, T. and Sears, W. R., "Airfoil Theory for Non-Uniform Motion," *Journal of Aeronautical Sciences*, Vol. 5, pp. 379–390, 1938.

Walker, G. J., "The Turbulent Boundary Layer on an Axial Compressor Blade," ASME Paper No. 82-GT-52, 1982.

Weinig, F., "Die Strömung um die Schaufeln von Turbomaschinen," *Johann Ambrosius Barth*, Munich, 1935.

Whitehead, D. S., "Force and Moment Coefficients for Vibrating Airfoils in Cascade," Aeronautical Research Council R and M 3254, February 1960.

Yeh, H. and Eisenhuth, J. J., "The Unsteady Wake Interaction in Turbomachinery and Its Effect on Cavitation," Transactions of the ASME, *Journal of Basic Engineering*, Series D, Vol. 18, No.2, pp. 181–189, June, 1959.

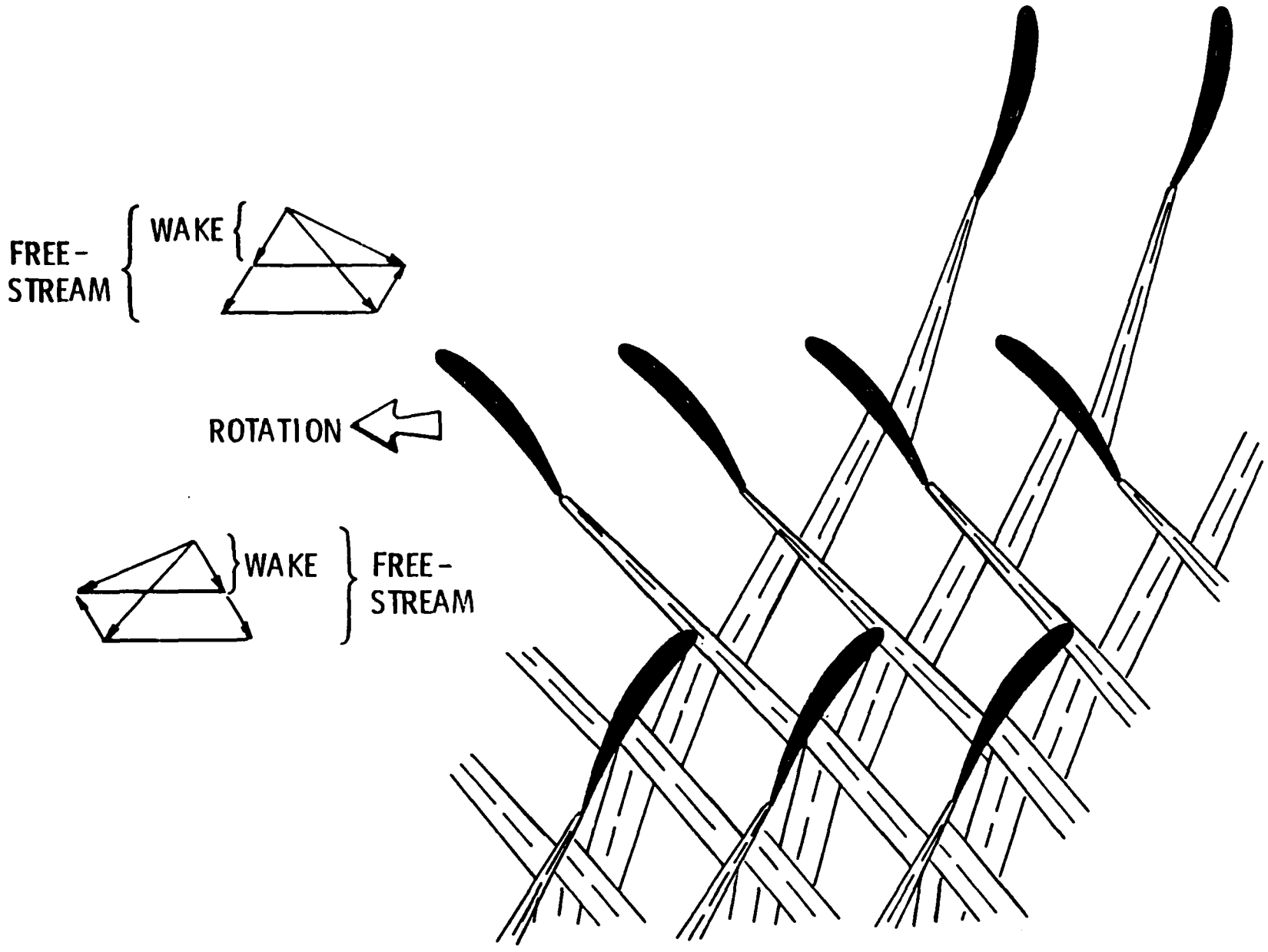

Figure 1. Periodic-average wake transport and interaction.

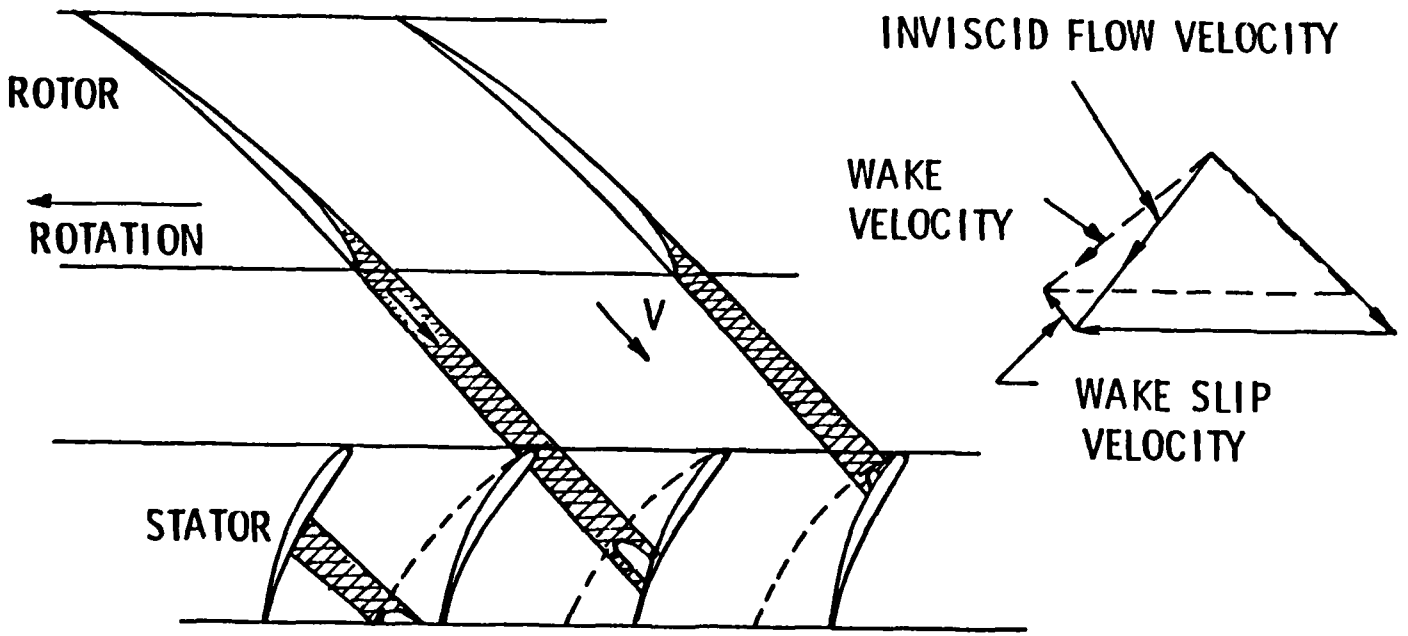

Figure 2. Transport of rotor wake segment through a compressor blade passage.

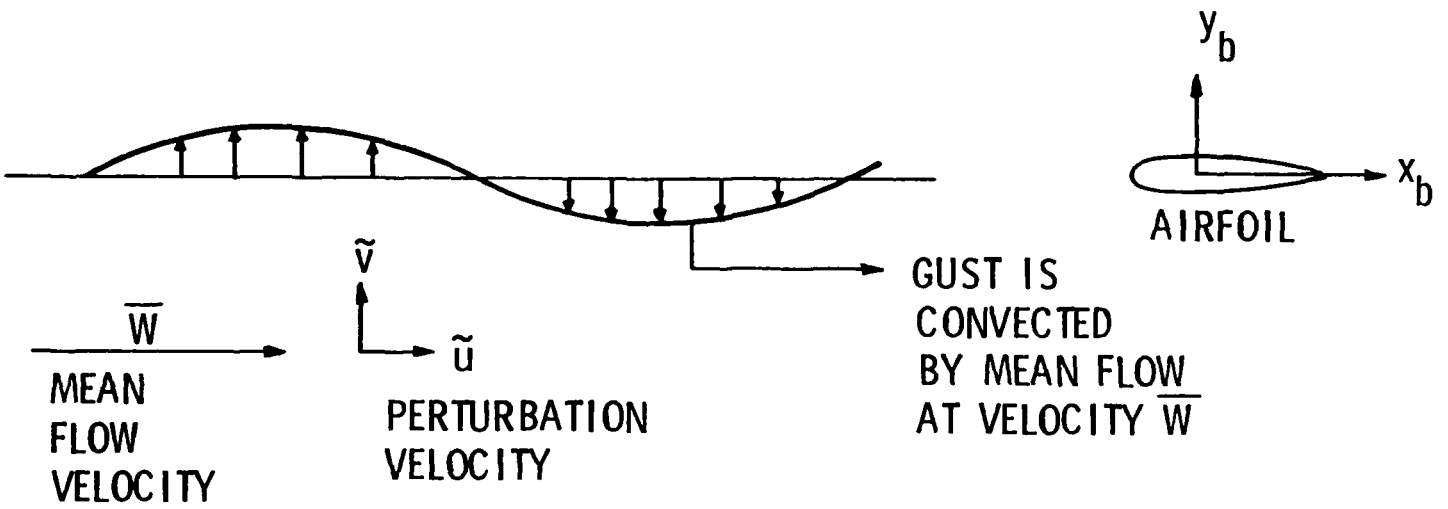

Figure 3. Transverse distortion velocity (Sears[1941]).

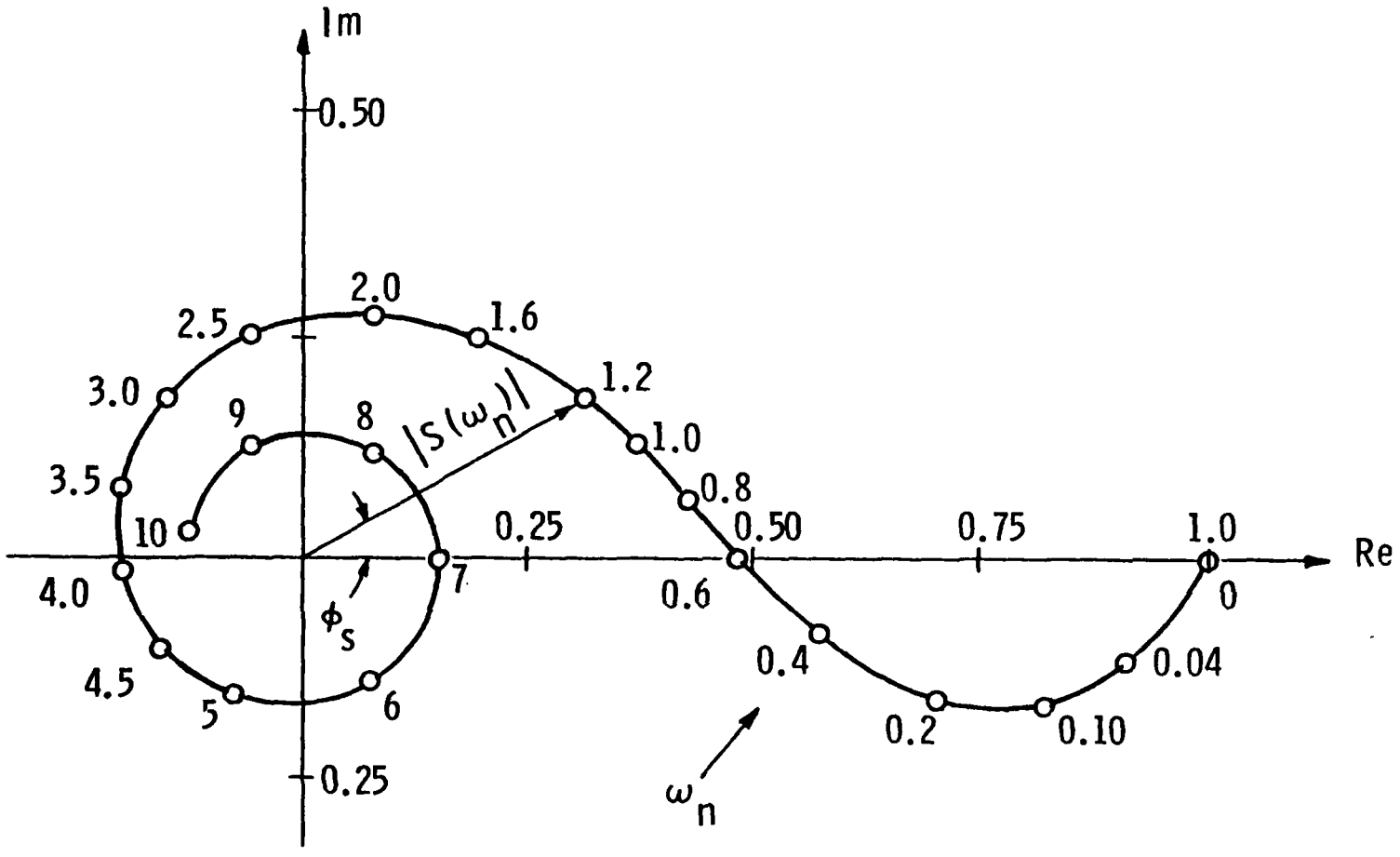

Figure 4. Sears Function.

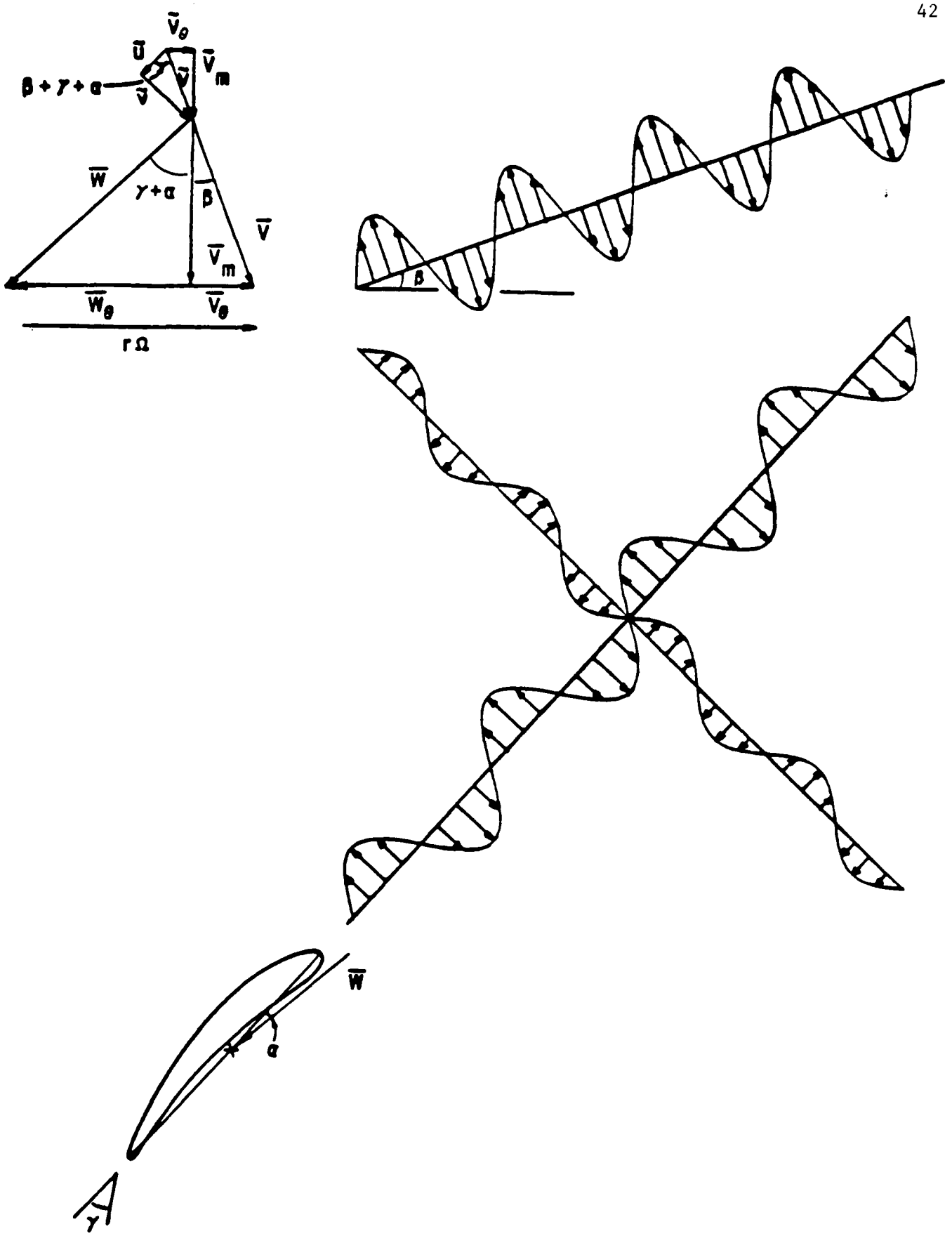

Figure 5. Decomposition of a distortion velocity into chordwise $\tilde{u}$, and transverse, $\tilde{v}$, components relative to the blade section.

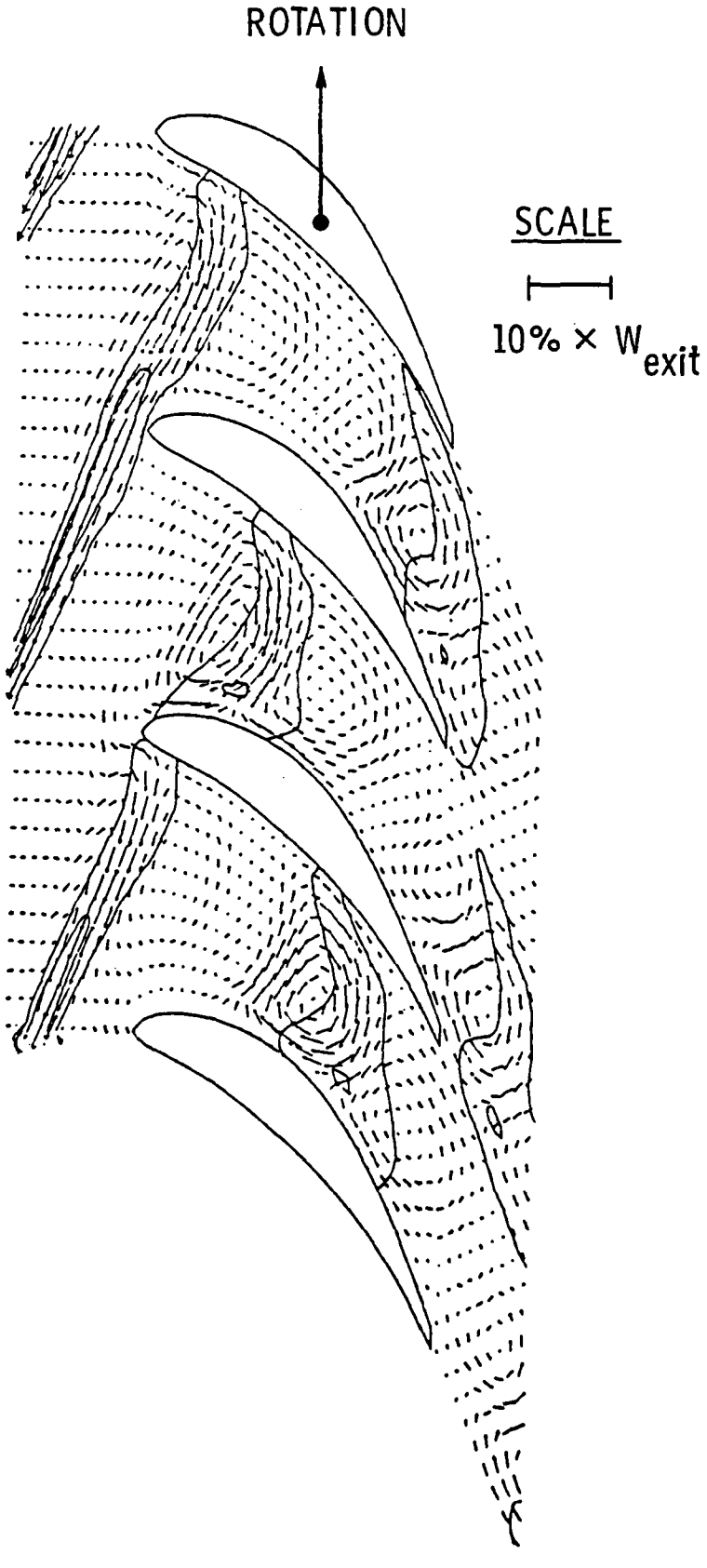

Figure 6. Wake-generated unsteady flow around a rotating turbine blade row.

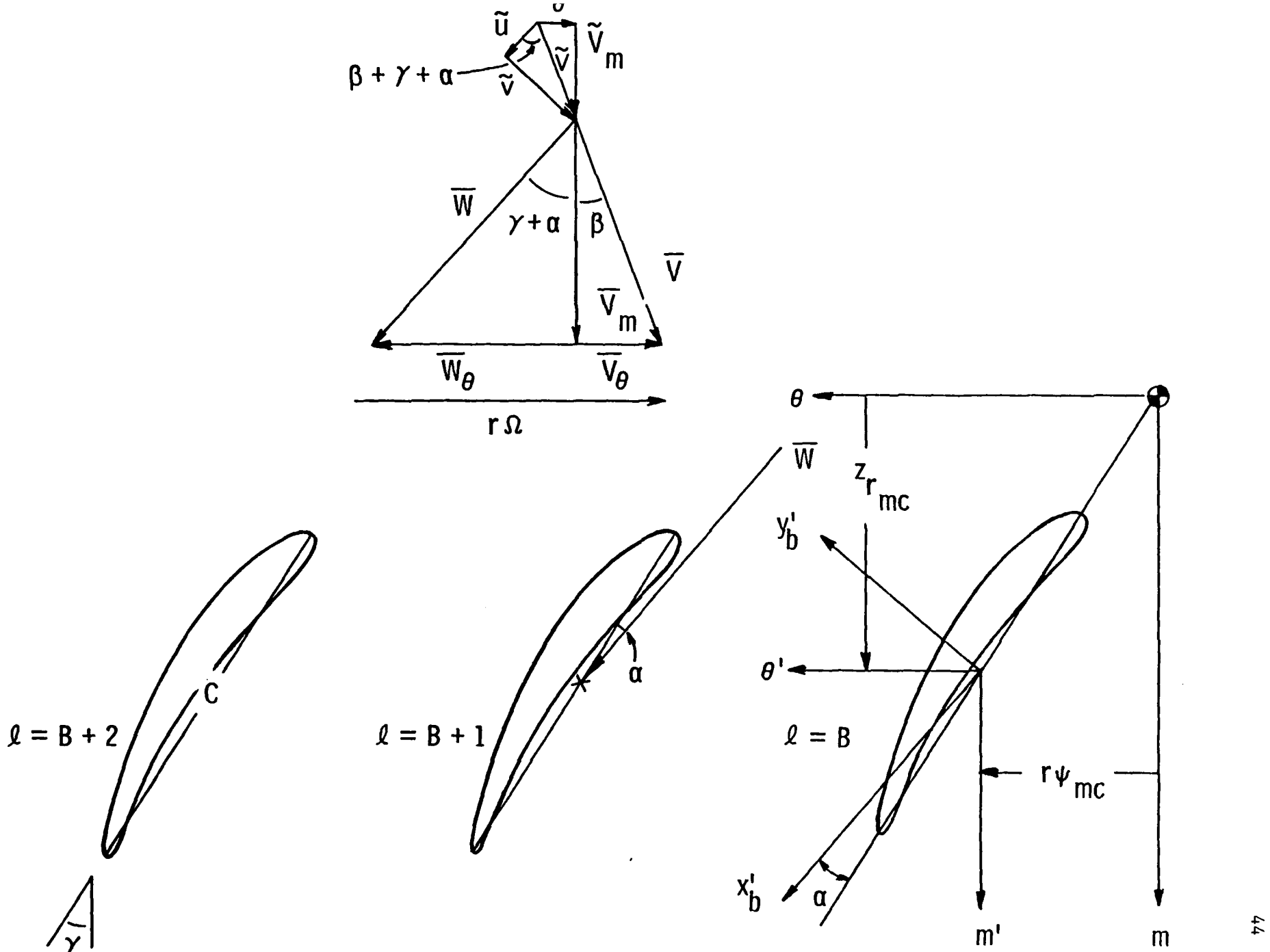

Figure 7. The rotating coordinate system with skew, ψ, and rake, z_r, defined at midchord (radial direction positive out of paper).

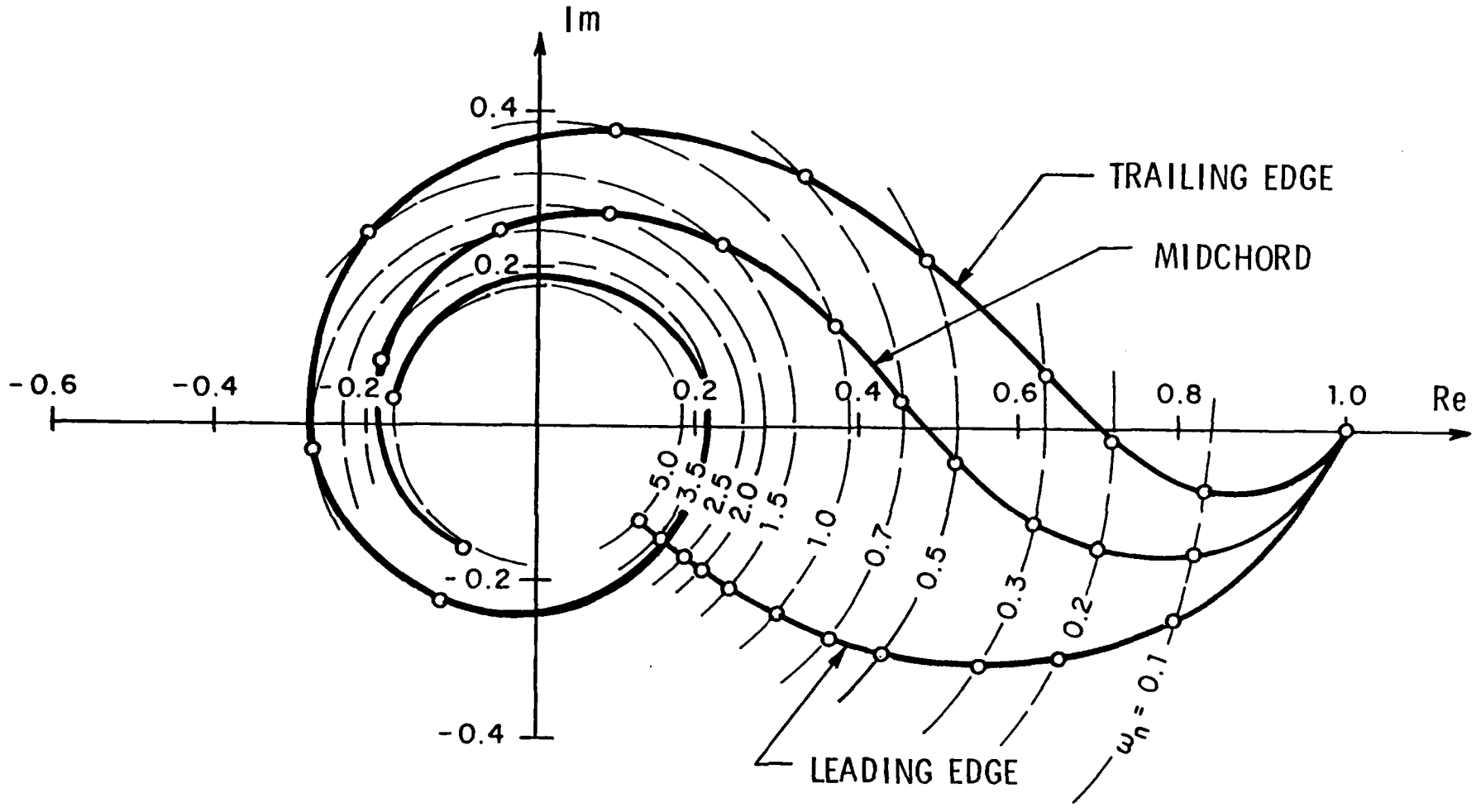

Figure 8. Unsteady lift coefficient function (Brown [1964]) defined with the coordinate system located at various blade locations. (The curves of constant reduced frequency, ω_n, are curves of constant unsteady lift amplitude).

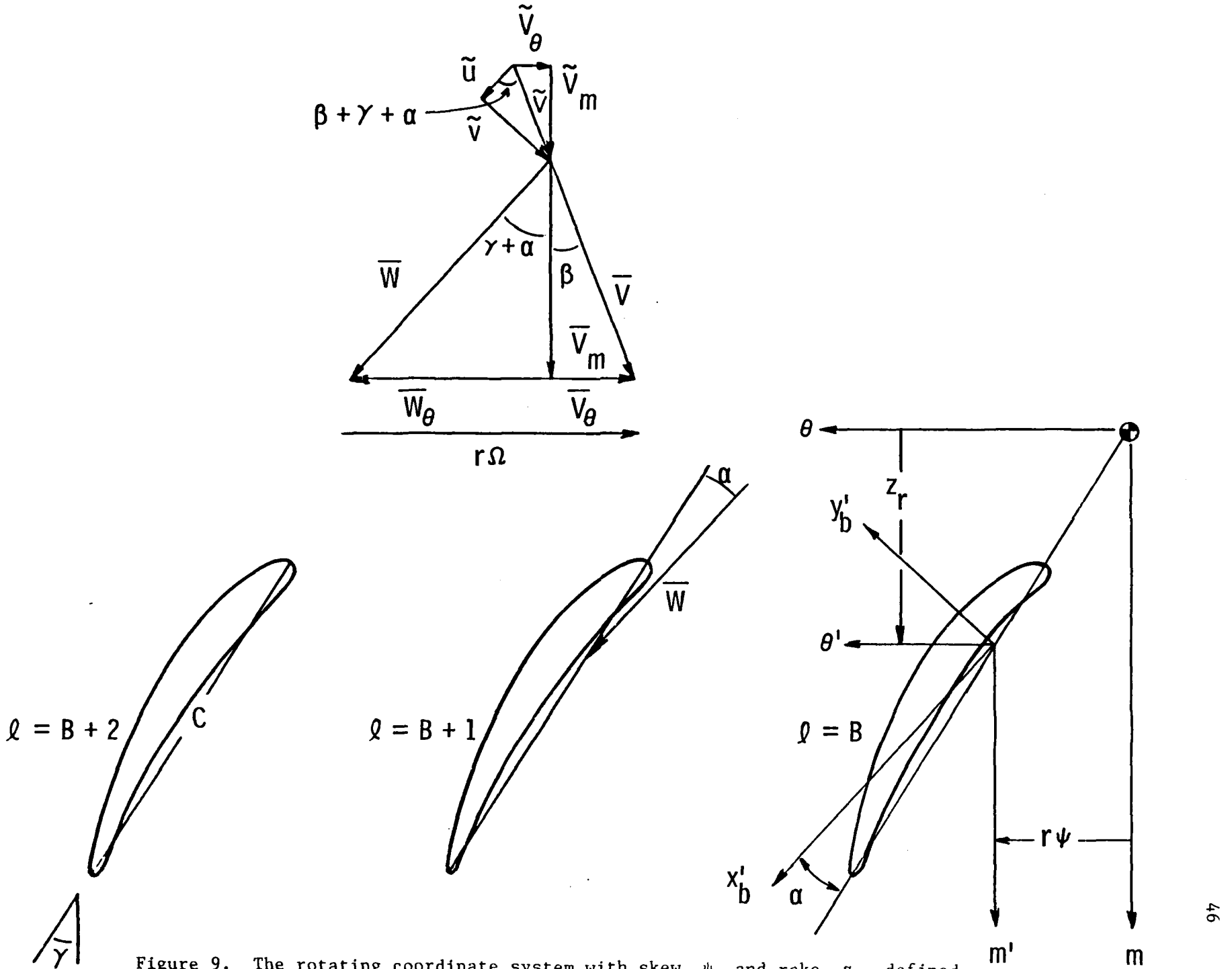

Figure 9. The rotating coordinate system with skew, ψ, and rake, z_r, defined as quarter chord (radial direction positive out of paper).

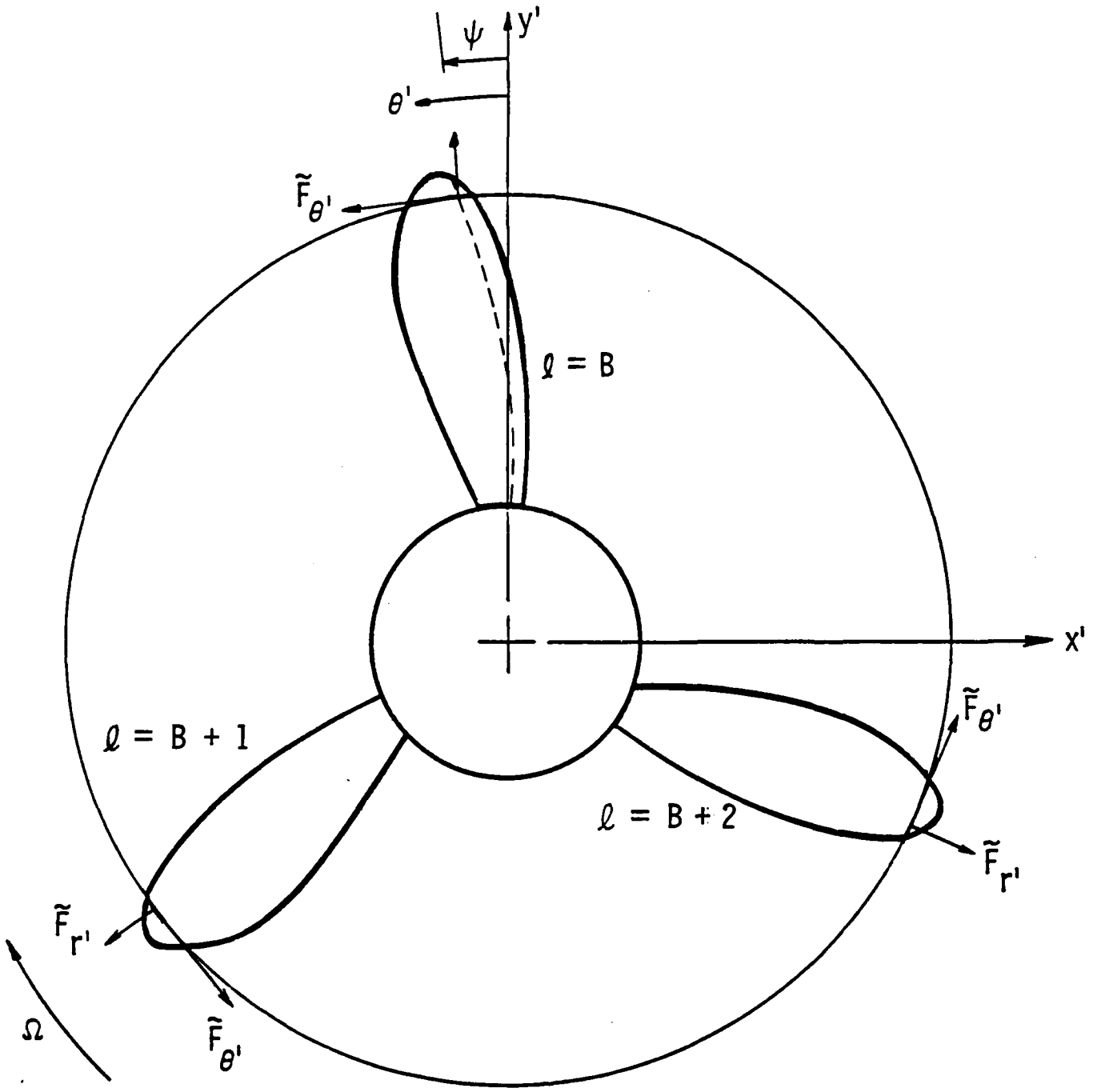

Figure 10. System used to resolve the unsteady lift force into components in the x' and y' directions (flow out of paper).

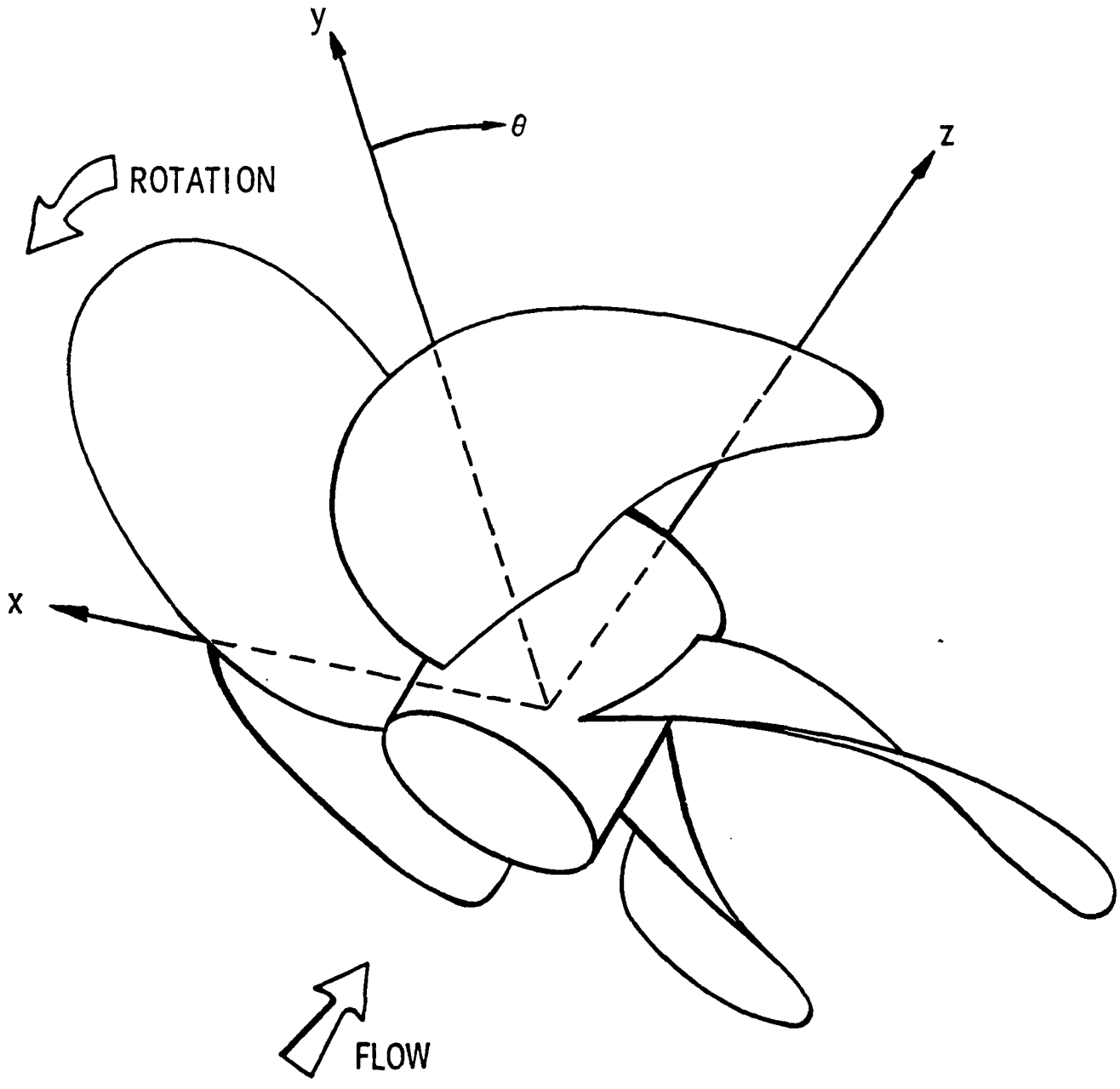

Figure 11. The stationary coordinate system.

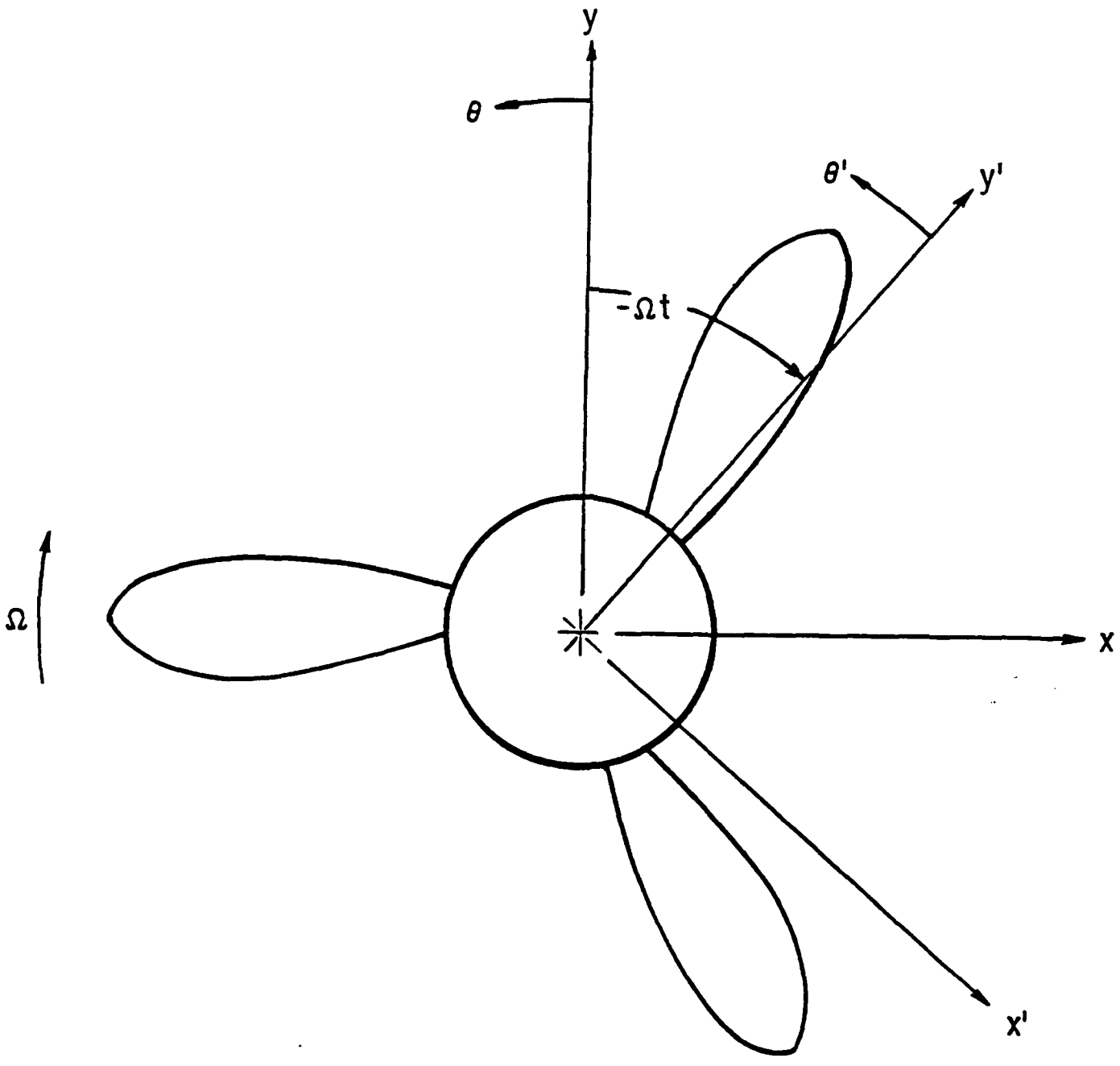

Figure 12. The rotating and stationary coordinate systems (flow out of paper with the radial direction taken from the hub centerline).